

INTERNATIONAL SOCIETY FOR SOIL MECHANICS AND GEOTECHNICAL ENGINEERING



This paper was downloaded from the Online Library of the International Society for Soil Mechanics and Geotechnical Engineering (ISSMGE). The library is available here:

<https://www.issmge.org/publications/online-library>

This is an open-access database that archives thousands of papers published under the Auspices of the ISSMGE and maintained by the Innovation and Development Committee of ISSMGE.

Laboratory Testing

Essais en Laboratoire

Chairman
Co-Chairman
General Reporter
Co-Reporter and
Tech. Secr.
Panelists

J.G. Zeitlen (Israel)
D.H. Shields (Canada)
P. von Soos (FRG)

G. Sällfors (Sweden)
A.S. Balasubramaniam (South East Asia), H.M. Jacobsen (Denmark), R.E. Olson (USA),
T. Ramamurthy (India), P.W. Taylor (New Zealand), C.P. Wroth (U.K)

T. Ramamurthy, Panelist

An attempt is made in this panel report to present prediction of strength, deformation and stress-strain response of a granular material in fully drained condition under plane strain from the data obtained by conducting drained axisymmetric compression tests using enlarged lubricated end platens. Use of such end platens result in near uniform deformations over the entire specimen with slender ratio equal to one. The importance of obtaining data under plane strain conditions cannot be overemphasised since large number of problems correspond to plane strain or near plane strain conditions, such as in earth dams, earth retaining structures, foundations, etc. In order to predict the performance of these structures, behaviour of soils need to be examined under plane strain. In most laboratories plane strain equipment does not exist and therefore, if relationships are established linking the behavioural pattern in axisymmetric compression to plane strain compression, this difficulty could be overcome and the analysis could be carried out with required degree of sophistication.

Some of the plane strain equipment in vogue

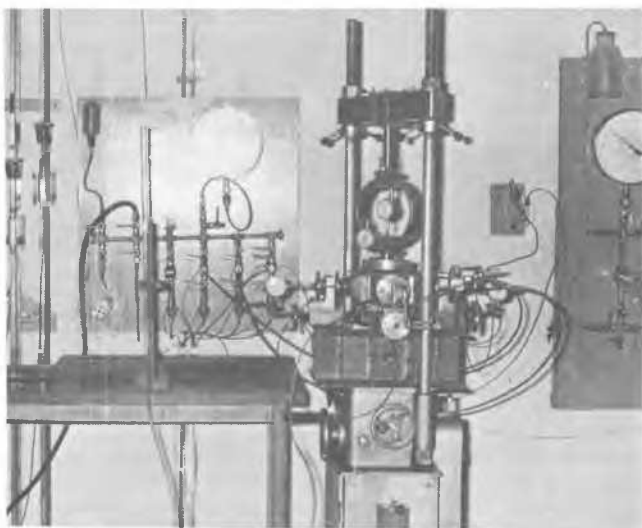


Fig. 1 Set up of Universal Triaxial Apparatus

have fixed, rigid lubricated plane strain faces, through which the intermediate principal stress could be applied and measured. Other equipment have flexible lateral faces and pressure on these faces is monitored by maintaining $\epsilon_2 = 0$, ϵ_2 being the intermediate principal strain. It is interesting to note that these systems adopted in maintaining plane strain condition do not significantly influence the performance behaviour of the specimens. (Ramamurthy et al, 1981).

At the Indian Institute of Technology, Delhi a Universal Triaxial Apparatus with flexible boundaries on the lateral faces has been in use for several years. (Ramamurthy, 1970, Rawat 1976, Shankariah 1977, Rawat and Ramamurthy, 1978). Figure 1 shows the entire set up of the Universal Triaxial Apparatus which can produce general stress conditions including plane strain condition.

Various researchers working with plane strain apparatus have established relationship between intermediate principal stress and other data obtained from this test. Bishop (1966) gave the following relationship.

$$(\sigma_2)_p = \frac{1}{2} (\sigma_1 + \sigma_3)_p \cos^2 \phi \quad (1)$$

The subscript p denotes values pertaining to plane strain condition and σ_1 , σ_2 , σ_3 are the major, intermediate and minor principal stresses.

Green (1971) found the following relationship valid for dense Ham River sand,

$$(\sigma_2)_p = \sqrt{(\sigma_1 \sigma_3)_p} \quad (2)$$

Working with Kaolin, Hamby and Roscoe (1969) gave the following expression

$$(\sigma_2)_p = s \left(\frac{18 - M^2 + 9n^2}{2(M^2 + 9)} \right) \quad (3)$$

$$\text{where } s = \frac{1}{2} (\sigma_1 + \sigma_3)_p$$

$$t = \frac{1}{2} (\sigma_1 - \sigma_3)_p$$

$$n' = t/s$$

$$\text{and } M = 6 \sin \phi_c / (3 - \sin \phi_c)$$

Ohta and Hata (1971) have suggested the following simple expression, for the case when 10% error is permitted,

$$(\sigma_2)_p = \frac{1}{2} (\sigma_1 + \sigma_3)_p \quad (4)$$

Parry (1971) has used a similar expression having the same form as equation (4).

$$(\sigma_2)_p = 0.4 (\sigma_1 + \sigma_3)_p \quad (5)$$

Based on a stress-dilatancy theory which takes into consideration the anisotropy of soil, Tatsuoka (1976) derived the following expression,

$$(\sigma_2)_p = K^{-1/(K+1)} \cdot (\sigma_1/\sigma_3)^{K/(K+1)} \cdot a^{1/(K+1)} \quad (6)$$

$$\text{where } K = \tan^2 (45 + \frac{1}{2} \phi_\mu)$$

ϕ_μ = Mean angle of interparticle friction

(σ_1/σ_3) = Stress ratio in plane strain

a = A factor taking anisotropy into consideration $= (d\epsilon_2/d\epsilon_3) < 1$ and obtained from axisymmetric triaxial test.

Finally from electro-plastic theory of Lade and Duncan (1975), putting $\epsilon_2 = 0$, Dickin and Brown (1977) have derived, for the plane strain case,

$$(\sigma_2)_p = \left(\frac{D+1}{D+R} \cdot \sigma_1 \right)_p \quad (7)$$

where D = Dilatancy factor

R = Stress ratio

σ_1 = Major principal stress

All above quantities refer to plane strain condition.

As seen from the relationships presented above there is no relationship from which $(\sigma_2)_p$ can be computed exclusively from the data of axisymmetric test.

From the large amount of data available in literature in addition to data obtained from Universal Triaxial Apparatus it has been noted that the ratio of mean stress to deviator stress, both at failure, in triaxial compression and plane strain are equal, i.e.

$$\left(\frac{\sigma_1 + \sigma_2 + \sigma_3}{\sigma_1 - \sigma_3} \right)_c = \left(\frac{\sigma_1 + \sigma_2 + \sigma_3}{\sigma_1 - \sigma_3} \right)_p \quad (8)$$

This can be simplified to

$$\frac{1}{\sin \phi_c} - \frac{1}{\sin \phi_p} = \frac{2}{3} b_p$$

$$\text{where } b_p = \left(\frac{\sigma_2 - \sigma_3}{\sigma_1 - \sigma_3} \right)_p$$

By adopting,

$$\left(\frac{\sigma_2}{\sigma_1 + \sigma_3} \right)_p = \frac{1}{2} \cos^2 \phi_p$$

We obtain,

$$\sin \phi_p + 3 \left(\frac{1}{\sin \phi_c} - \frac{1}{\sin \phi_p} \right) = 1 \quad (9)$$

Further, by adopting

$$(\sigma_2)_p = \sqrt{(\sigma_1 \sigma_3)_p}$$

We obtain,

$$3 \sin \phi_p - \sin \phi_c (\sin \phi_p + \cos \phi_p) = 2 \sin \phi_c \quad (10)$$

Equations (9) and (10) connect the triaxial compression strength to plane strain strength. It has been found that equation (9) is valid for loose sands which show small or zero dilation while equation (9) is valid for dense soils which show large dilation at failure. In order to calculate the plane strain strength at any relative density, the following equation gives good agreement,

$$\phi_p = 1.42 (\phi_{p10} - \phi_{p9}) (I_D - 0.25) + \phi_{p9} \quad (11)$$

where ϕ_p = plane strain strength at the desired relative density (I_D expressed as fraction)

ϕ_{p9} and ϕ_{p10} refer to ϕ_p calculated according to equations (9) and (10) respectively.

From above, by use of equation (11) and (8) it is possible to calculate the major and intermediate principal stresses for plane strain condition from the result of only triaxial compression test (Ramamurthy and Tokhi, 1981).

It has been observed by the examination of large amount of available data that the ratio of lateral strain to axial strain in plane strain at failure can be conveniently expressed by the following empirical expression, (Tokhi and Ramamurthy 1980)

$$\left(\frac{\epsilon_3}{\epsilon_1} \right)_p = \cos^2 \phi_p - 1.71 \quad (12)$$

From the critical examination of experimental results of various investigators it has been found that the ratio of failure axial strain in triaxial compression to that in plane strain is a function of ratio of mean stress and principal stress ratio at failure in the two

test conditions. The following expression gives good agreement with the experimental results,

$$\frac{(\epsilon_{1f})_c}{(\epsilon_{1f})_p} = \frac{(\sigma_m)_p}{(\sigma_m)_c} \cdot \frac{R_p}{R_c} \quad (13)$$

where

R_c = Principal stress ratio (σ_1/σ_3) at failure in triaxial compression

R_p = Principal stress ratio (σ_1/σ_3) at failure in plane strain.

$(\sigma_m)_c$ = Mean stress at failure in triaxial test $= (1/3)(\sigma_1 + 2\sigma_3)_c$

$(\sigma_m)_p$ = Mean stress at failure in plane strain test calculated as equal to $(1/3)(\sigma_1 + \sqrt{\sigma_1\sigma_3} + \sigma_3)_p$

Also in plane strain the failure ratio (R_f) as defined by Duncan and Chang (1970) in hyperbolic stress strain formulation suggested by Kondner and Zelasko is given by the following expression,

$$\frac{(R_f)_c}{(R_f)_p} = 1.71 - \cos^2 \phi_p \quad (14)$$

It has also been observed that the stress strain response in plane strain upto failure is essentially hyperbolic in nature.

From the foregoing, by the use of equations 11, 13 and 14, and the results of triaxial compression test, it is simple to calculate $(\sigma_1 - \sigma_3)_{fp}$, $(\epsilon_{1f})_p$ and $(R_f)_p$. With these it is possible to predict the stress-strain response in plane strain (Tokhi 1981). Figure 2 shows the transformed plot of ϵ_1 versus $\epsilon_1/(\sigma_1 - \sigma_3)$ in plane strain. Since $(\sigma_1 - \sigma_3)_{fp}$ and $(\epsilon_{1f})_p$ are predicted, the failure point A can be located. Also since $(R_f)_p$ can be predicted, the slope of the straight line passing through A ($b' = b'$) on the transformed plot is given by

$$b' = (R_f)_p / (\sigma_1 - \sigma_3)_{fp} \quad (15)$$

Knowing b' , the intercept a' which is inverse of initial tangent modulus ($b = OB$) is given by from figure 2 as

$$a' = 1/(\epsilon_1)_p = \epsilon_{1fp} (1 - R_{fp}) / (\sigma_1 - \sigma_3)_{fp} \quad (16)$$

The line AB represents the stress-strain relationship in plane strain on the transformed plot. The deviator stress versus axial strain can then be computed from the following equation.

$$(\sigma_1 - \sigma_3) = \epsilon_1 / (a' + b' \epsilon_1) \quad (17)$$

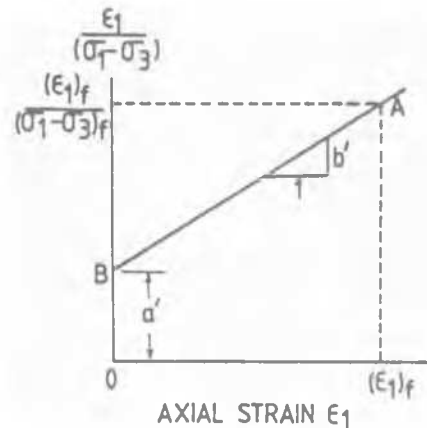


Fig. 2 Transformed plot ϵ_1 versus $\epsilon_1/(\sigma_1 - \sigma_3)$ for plane strain condition

Figure 3 shows the predicted stress strain curves in plane strain using the data from axisymmetric compression tests. The experimental data are also shown in these figures. Large number of data is available, but only a few predictions from a wide range of researchers are included in this figure to emphasise the successful application of the theory outlined above.

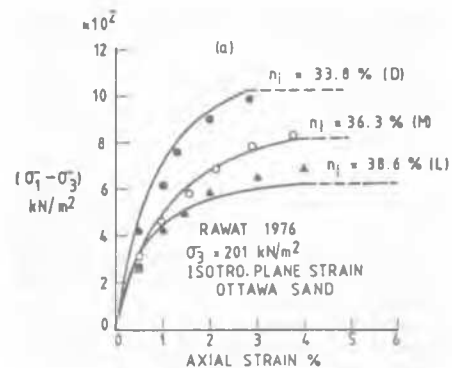


Fig. 3(a): Predicted curves for plane strain condition from data of axisymmetric compression test, (n_i = Initial porosity, D = Dense, M = Medium dense, L = Loose)

Examination of large data published on axisymmetric compression ($b = 0$) and extension ($b = 1$) strengths obtained from specimens tested with usual precautions to produce condition of near uniform deformation in the entire specimen and also the plane strain strength data, it has been observed that

$$\phi_c < \phi_p > \phi_e$$

and

$$\phi_c \leq \phi_e$$

$|\phi_c - \phi_e|$ is essentially due to anisotropy, introduced during deposition, particle shape and whether the mean stress is increasing,

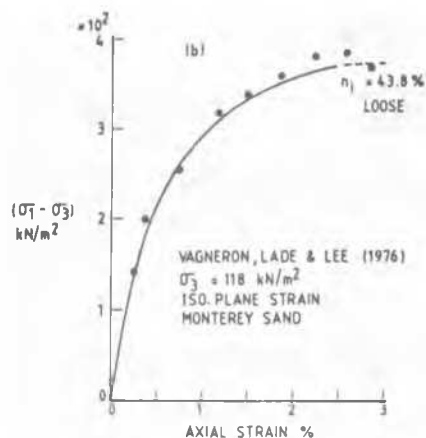


Fig. 3(b): Predicted curves for plane strain condition from data of axisymmetric compression test. (Iso = Isotropically consolidated specimen, n_1 = Initial porosity).

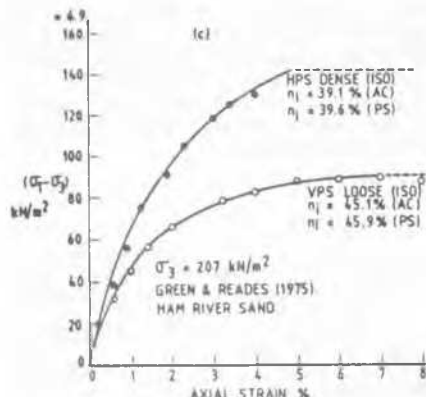


Fig. 3(c): Predicted curves for plane strain condition from data of axisymmetric compression test:
HPS Horizontal plane strain
VPS Vertical plane strain
AC Axisymmetric compression
PS Plane strain
Iso Isotropically consolidated specimen

decreasing or remaining constant in extension compared to that in compression test. It has been clearly brought out by Tokhi and Ramamurthy (1981) that ϕ_e obtained from axisymmetric triaxial tests using enlarged and lubricated end platens should be treated as reliable since the specimen deforms under least lateral constraints and that throughout the range $0 < b < 1$, ϕ_p is the maximum strength.

This behaviour could be represented in two stages, one from $b = 0$ to $b = b_p$ (i.e. upto plane strain) and another from $b = b_p$ to $b = 1$.

Examination of large data of such behaviour enabled to represent this behaviour in the following forms (Tokhi, 1981). In the region $0 < b < b_p$

$$\sin \phi_b = \sin \phi_c + (\sin \phi_p - \sin \phi_c) \left(\frac{b}{b_p} \right)^n \quad (18)$$

and in the region $b_p < b < 1$,

$$\sin \phi_b = \left[\sin \phi_p - (\sin \phi_p - \sin \phi_e) \cdot \left(\frac{b - b_p}{1 - b_p} \right)^{n'} \right] \quad (19)$$

A representative value of $n = 0.6$ and $n' = 1.4$ gives good agreement with experimental data of several researchers. An empirical value of b_p as follows is used in above equations,

$$b_p = 0.535 - 0.000625 \phi_c^* \quad (20)$$

Out of large data interpreted according to above a few curves are shown in Figure 4 which show the plot of equations 18 and 19 indicated by solid lines. Experimental points are also shown and a good agreement is suggested.

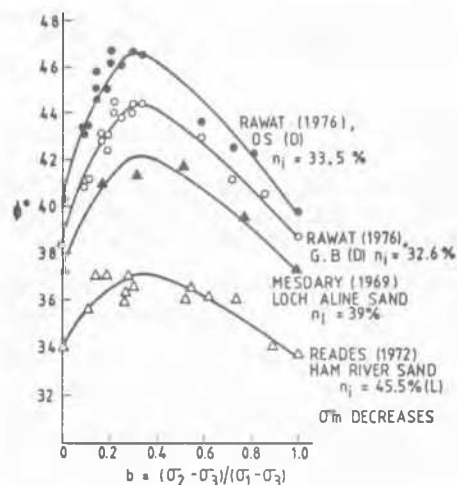


Fig. 4: Predicted relationship showing variation of ϕ versus b

In conclusion this report has attempted to highlight three points that by simple procedures it is possible to predict (i) the plane strain strength (ii) the stress-strain curve in plane strain from data of axisymmetric tests alone and (iii) a new approach is presented in defining a failure criteria in a manner that minimizes the deviation of strength at any value of b and the experimentally determined strength. The failure criteria is definable by experimentally determining ϕ_c , ϕ_e and ϕ_p .

When proper equipment for determination of ϕ_p is not available, its value can be predicted as explained earlier.

The author wishes to express his gratitude to Mr. Tokhi for his help at every stage in the preparation of this report.

References

- Barden, L., Khayatt, A.J. and Wightman, A. (1969). Elastic and slip components of deformation of sand. *Canadian Geotech. Jnl.* Vol. 6, No. 3, 227-240.
- Barden, L. and Proctor, D.C. (1971). The drained strength of granular material. *Canadian Geotech. Jnl.* Vol. 8, No. 3, 372-383.
- Bishop, A.W. (1966). The strength of soils as engineering materials (6th Rankine Lecture) *Geotechnique*, Vol. 16, No.2, 91-128.
- Cornforth, D.H. (1964). Some experiments on the influence of strain conditions on the strength of sand. *Geotechnique*, Vol. 14, No. 2, 143-167.
- Duncan, J.M. and Chang, C.Y. (1970). Non linear analysis of stresses and strains in soils. *Jnl. of soil mech. and found. div. ASCE* Vol. 96, No. 5, 1629-1652.
- Dickin, E.A. and Brown, A.J.P. (1977). Discussion *Jnl. of Soil Mech. and Found. Div. ASCE* Vol. 103, No. 1, 68-70.
- Green, G.E. (1971). Strength and deformation of sand measured in independent stress control cell. *Proc. Roscoe memorial Symposium, Cambridge*, 285-323.
- Hambly, E.C. and Roscoe, K.H. (1969). Observations and predictions of stresses and strains during plane strain of 'wet' clay *Proc. 7th Int. Conf. Soil Mech. and Found. Engg. Mexico*, Vol. 1, 173-181.
- Kondner, R.L. and Zelasko, J.S. (1963). A hyperbolic stress strain formulation for sands. *Proc. second Pan American Conf. Soil Mech. and Found. Engg.* 289-324.
- Lade, P.V. and Duncan, J.M. (1975). Elasto-plastic stress-strain theory for cohesionless soil. *Jnl. of Geotech. Engg. Div. Proc. ASCE*, Vol. 101, GT 10, 1037-1053.
- Ohta, H. and Hata, S. (1971). Plane strain stress-strain relations for soils. *Proc. Fourth Asian Reg. Conf. Soil Mech. and Found. Engg. Bangkok*, Vol. 1, 57-62.
- Parry, R.H.G. (1971). A study of the influence of intermediate principal stress on O' values using a critical state theory. *Proc. Fourth Asian Reg. Conf. Soil Mech. and Found. Engg. Bangkok*, 159-165.
- Ramamurthy, T. (1970). A Universal triaxial apparatus. *Jnl. of Indian National Society of Soil Mech. and Found. Engg.* Vol. 9, No. 3, 251-269.
- Ramamurthy, T., Rawat, P.C. and Tokhi, V.K., (1981). Plane strain behaviour of granular medium under submission to *Indian Geotechnical Jnl.* Vol. 11, No. 4.
- Ramamurthy, T. and Tokhi, V.K. (1981). Relation of triaxial and plane strain strengths. *Proc. 10th Int. Conf. Soil Mech. and Found. Engg. Stockholm*, Vol. 1, 755-758.
- Rawat, P.C. (1976). Shear behaviour of cohesionless materials under generalized conditions of stress and strain. *Ph.D. Thesis, I.I.T. Delhi*.
- Rawat, P.C. and Ramamurthy, T. (1978). Shear behaviour of sand under generalized conditions of stress and strain. *Indian Geotech. Jnl.* Vol. 8, No. 4, 235-269.
- Shankariah, B. (1977). Behaviour of anisotropic granular media under general stress systems. *Ph.D. Thesis, I.I.T. Delhi*.
- Sutherland, H.B. and Mesdary, M.S. (1969). The influence of intermediate principal stress on the strength of sand. *Proc. 7th Int. Conf. Soil Mech. and Found. Engg. Mexico*, Vol. 1, 391-399.
- Tatsuoka, F. (1976). Stress dilatancy relations of anisotropic sands in three dimensional stress condition. *Soils and Foundations*, Vol. 16, No. 2, 1-18.
- Tokhi, V.K. and Ramamurthy, T. (1980). Evaluation of strength parameters for plane strain problems. *Proc. GEOTECH-80*, Vol. 1, 45-49.
- Tokhi, V.K. and Ramamurthy, T. (1981). Discussion on 'An evaluation of three dimensional shear testing'. *Proc. 10th Int. Conf. Soil Mech. and Found. Engg. Stockholm*, Vol. 4.
- Tokhi, V.K. (1981). Relationship between strength and stress-strain behaviour in triaxial compression and plane strain. *Ph.D. Thesis (under submission to I.I.T. Delhi)*.
- Vagneron, J., Lade, P.V. and Lee, K.L. (1976). Evaluation of three stress-strain models for soils. *Proc. Second Int. Conf. on numerical methods in Geomechanics, Virginia*, Vol. 3, 1329-1351.

H. Moust Jacobsen, Panelist

TWO COMMENTS ON LABORATORY TESTS

Triaxial tests are widely used to day and many of the contributions to this conference present theories based on such tests. But interpretation of triaxial test results is problematic and use of other test types should be taken under consideration.

The first comment deals with the inclined failure surface, which develops especially in firm soils, more seldom in weak soils. Let us consider a pre-consolidated clay with well known properties, even before sampling (fig. 1). The drained

strength is smaller than the undrained strength, so it is an unstable soil. For large strains critical states occur, q and e_v get constant for constant value of p . (q is the deviation stress, e_v the volumetric strain, and p the total, mean normal strength.)

This soil will now be investigated in an undrained triaxial test with the height of the specimen twice the diameter. Initially the test result follows the undrained performance curve. But when q increases the soil will try to expand. It should

be impossible since the drains are closed. But inside the sample water flows from some parts which get stiffer to some parts which get weaker. The test is not undrained any longer (fig. 2).

As the drained zone develops it dominates the performance curve. The strains should be calculated by using the unknown width of the zone instead of the height of the sample, so ϵ_1 becomes wrong too (fig. 3). Inside the drained zone the critical state develops in a narrow band as the test goes on. The wellknown failure surface appears at the surface of the sample, and the dominating stress state is now plane instead of triaxial (fig. 4).

The measured curve has very little to do with the real properties of the soil. Every time a distinct failure surface appears during the tests, the result should normally not be used to scientific purposes. So the main problem as illustrated in this example is to ensure that *theories do not reflect test errors but the real properties of the soil*.

The second comment deals with the choice of laboratory tests on soil elements. When using samples, which height equals the diameter, and observing homogeneously distributed strains, we got nearly correct results (fig. 1). But today we have realized that the axisymmetrical state is very special and does normally not occur in the nature. For practical purposes we therefore have to correct the triaxial results by means of complicated theories.

It is, however, possible to avoid corrections of test results by analyzing the stress and strain states in the actual case and then choose a laboratory equipment, which fulfils the stress and strain conditions. Some examples are shown in the table. The use of the triaxial apparatus will then be reduced essentially. It is still convenient for studying basic phenomena but the plane strain apparatus is proposed to replace it in most problems.

In stability problems failure often takes place in narrow bands and in that case tests with distinct failure surfaces should be used to measure the residual strength of the soil.

Table 1. Use of laboratory tests

- | | |
|--|--|
| 1. Settlement calculations
e.g. Oedometer tests | |
| 2. Study of basic phenomena
e.g. Triaxial tests ($H = D$) | |
| 3. Stress-strain relationships
Homogeneous specimens:
e.g. Plane strain tests ($H = D$)
True triaxial tests | |
| | 4. Stability problems
Narrow band tests
e.g. Triaxial tests ($H = 2D$)
Shear box tests
Plane strain tests ($H = 2D$) |
| | 5. Other practical problems
e.g. Plane strain tests ($H = D$) |

Fig. 1.

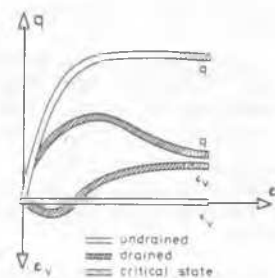


Fig. 2.

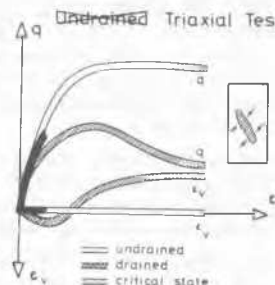


Fig. 3.

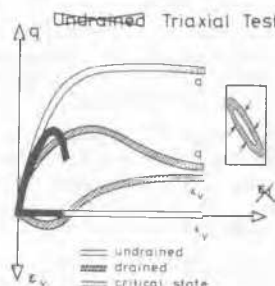
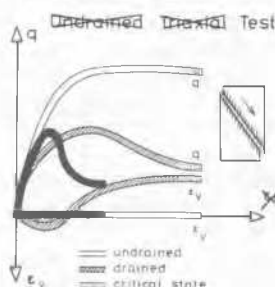


Fig. 4.



A.S. Balasubramaniam, Panelist

Mr. Chairman, Ladies and Gentlemen, at the very outset I would like to congratulate the General Reporter, Mr. P.V. Soos and the Co-Reporter, Mr. G. Salfors for their excellent report summarizing the 64 papers presented in this session and to highlight them from other related publications. It is indeed an enormous task, when one considers the wide range of topics that are covered in these papers, when compared to the original intention of having contributions on relevance of laboratory testing; standardization of laboratory testing for practical applications, new laboratory testing methods; and, model tests.

The papers presented herein include almost all the aspects of soil mechanics starting from index tests, activity and soil classification; seepage and permeability; effective stress principle of partially saturated soils; in-situ stress and K_0 determination; compaction; California Bearing Ratio; consolidation; swell, shrinkage and soil freezing; strength and deformation; and cyclic loading. These properties seem to have been studied on a wide range of materials such as sand with different relative density, clays with different consistency and sensitivity, mixed soil with grain size distribution varying from clay size to crushed rock. Also, included herein are soils of different geological origin and characteristics such as residual soils, expansive soils, soft rocks, mudstones, tuff, etc. With the exception of hard rock, all other materials seem to have been mentioned in one way or another. Moreover, in carrying out this study many types of apparatus new and old have been used and these include Swedish fall cone, ring shear apparatus, pressuremeter, oedometer standard and modified, simple shear, direct, shear, biaxial, standard and truly triaxial apparatus, and also centrifuge, among many others. Even in a typical apparatus such as the standard triaxial, samples of many sizes are being tested in a variety of manner under UU, CIU, CAU, CID, and CAD conditions. An impressive list of material behaviour such as swell, shrinkage, friction, fracture, elasticity, plasticity, creep, rheology, isotropy, anisotropy and several others are discussed at various levels of sophistication. Mention should also be made of the theories described, such as the failure criteria of the Extended Tresca type, critical state concept of Roscoe Schofield and Wroth, Cam Clay Theory of Schofield and Wroth, Hvorslev failure criterion, Barron's theory of equal strain and also Delay Models and Memory concepts. Thus I am fortunate to have read and learned a lot from the contributed papers.

At the same time, I wonder whether laboratory testing has to be considered as an exercise which provides relevant soil properties or parameters, to be determined from artificially prepared, or, on undisturbed samples taken from in-situ conditions under careful sampling. Tests on artificially prepared samples are often conducted under controlled conditions, even though, they do not represent many of the characteristics exhibited by natural deposits. Such tests are often carried out to develop simple theories which can be subsequently modified to incorporate many field conditions, and, are of the form that most engineers can understand, and, use them in their site investigation and design work, to reduce the expenses in carrying out an extensive series of tests. Thus, we are fortunate if a particular theory can be used to evaluate a few soil parameters which can describe a certain phenomenon to a reasonable degree of accuracy. Terzaghi's theory of consolidation is a classical

example, where, even though the theory is not adequate to take care of many phenomena such as secondary consolidation, aging, anisotropy etc., yet the theory is used almost in all instances to estimate the primary consolidation settlement for a first degree of approximation. At present, our confidence in taking good quality undisturbed samples extend only to homogeneous clays and as such laboratory tests to evaluate soil parameters need to be sophisticated in avoiding possible experimental errors. Similarly, refined theories can also be applied in design works. It is thus clear that the degree of sophistication applied should have the same weightage related to sampling, testing and in using theories.

Soil mechanics related to soft and stiff clays are now well advanced and it seems from the work of Bjerrum, Casagrande, Peck, Skempton and others, basic properties as derived from index tests and clay fraction (activity) can never be imagined to disappear or even be improved in soil classification and in estimating strength and compressibility parameters. Bjerrum in particular has used index properties extensively in soft clays to identify the stress history, undrained strength and even to the extent of correlating safety factors with plasticity index. On the other hand there still remains and enormous amount of soil deposits such as residual soils, expansive soils, dispersive soils, collapsible soils etc., among others for which such empirical correlations are not yet available for practising engineers. I am glad to note that at least a few papers in this session are devoted to the study of soils other than clays and in particular compacted and partially saturated soils. Our ability to take good quality samples in these materials and to test them in the laboratory to evaluate useful parameters have a long way to go before it can reach the same level of development as that has been achieved in soft and stiff clays. We are at present discussing the correlation of the behaviour of sand samples as tested in the plane strain apparatus, truly triaxial apparatus and in standard triaxial apparatus, when the only test that seem to be carried out in sand deposits in many parts of the world today is the Standard Penetration Test or the cone penetration test which are purely empirical in nature. We are indeed even discussing the role of yield function, plastic potential and normality rule in successfully describing the stress-strain behaviour of laboratory prepared sand specimens, when undisturbed sample of sand is yet in its early stage in many countries.

Another area which is not well developed is related to construction materials. An enormous amount of soil and crushed rock are used in construction related to highways, rail roads, embankments, and other types of dams. Of the sixty four papers presented in this session only a handful deal with this important area of research in which, after all, a large sum of money is currently spent in developing countries. The difficulty seems to lie in the availability of large scale testing devices in most of the laboratories. More laboratory testing methods are to be developed to test large size materials.

In the development of the stress-strain theories, the critical state concept developed by Roscoe, Schofield and Wroth and the associated stress-strain theories have recently been used extensively on many types of soils and has also been modified to take care such aspects as anisotropy, repeated loading, etc. Only a few papers in this session seem to apply these concepts for soft rocks, mudstones etc. and also to the behaviour under cyclic loading. I do agree with the reporters when they mentioned that their comments

are at times critical in the hope they will stimulate discussion during the conference. I thus disagree with their opening statement in Section 5.1.3 which says, since critical state soil mechanics was introduced in the early 60's much effort has been made to prove or disprove the theory. The critical state concept as developed in 1958, opened up a new line of thinking to soil engineers who have been long stagnated with Mohr circle of stresses and strength. Much of the work done in 60's is to establish critically the potential of the theory, and, methods by which it can be applied on undisturbed samples for engineering practice. In the last international conference held in Tokyo in 1977 more than two-thirds the published papers in the session on stress deformation of soils refer to the critical state concept and its application in a wide range of materials. Currently, most institutions in many parts of the world are actively engaged in developing stress-strain laws for soils and rocks. Indeed, the simplified yield loci presented by Larsson & Salfors for the Swedish clay is one such application. On the other hand, the work of Wen-Xi-Huang, Jia Lin Pu and Yu Jiong Chen in Peoples Republic of China are extensions of the flow rule and the normality concept adopted by Schofield and Wroth.

Many types of soil deposits are being extensively studied and in the case of Soft Clays, especially the Bangkok Clay, Scandinavian Clays, the Sensitive Canadian Clays and the Boston Blue Clay are a few to be mentioned. A large volume of data collected for nearly two decades, has enabled the analysis to be carried out using various types of statistical methods including the higher order regression analysis such as the factor analysis. Such analysis seems to indicate that most soil properties such as undrained strength, preconsolidation pressure, compression index etc., can be modelled as probability distributions which can be easily incorporated in settlement and stability analysis to yield the latter in the form of probability functions. It is thus now possible to quantify the uncertainties involved in the settlement and stability analysis. Considerable scatter is noted in many of the experimental data presented in this session and it appeared even simple regression analysis is not carried out to obtain the best fit curve to the test data. Also, the order of magnitude of the scatter in the test data seems to outweigh the refinement that can be obtained by investigating such phenomena as anisotropy, creep, etc. Statistical concept and data analysis are now being increasingly used in all branches of civil engineering.

An additional point to be emphasized is the errors and limitations of testing devices. Many standard equipment such as the triaxial apparatus or the oedometer has been in existence for nearly three decades and their possible errors and limitations are being investigated extensively. Such investigations

P.W. Taylor, Panelist

DYNAMIC SOIL TESTING

I wish to make three points concerned with the laboratory determination of dynamic soil properties.

My first point is concerned with the changes in pore water pressure in saturated cohesive soils during cyclic triaxial tests. I am not concerned here with the difficulties in measuring these changes, which are considerable.

In harmonic strain-controlled triaxial tests at ampli-

are also to be extended to the new equipment developed in the recent past to evaluate the uniformity in stresses, strains and other properties that are being measured.

While reading many of the papers presented here and elsewhere it appears that ISSMFE should as far as possible standardize not only the testing devices and testing procedures but also the type of notations and terminology that are used in common practice. Even though there are standard notations, it seems they are not strictly adhered to in the publications. When it comes to terminology, it is still a worse situation. A non-soil mechanics engineer is often confused with maximum past pressure, apparent maximum past pressure, preconsolidation pressure, critical pressure, yield stress, apparent preconsolidation pressure, quasi-preconsolidation pressure, geological preconsolidation pressure, etc. I wonder whether at some stage these pressures and other similar quantities be well defined without any ambiguity.

Since the model pile tests carried out by Whittaker on pile groups at the Building Research Establishment in U.K. in 1963, the only other model test which has opened up applications in practice very widely is the centrifugal model test. Professor Andrew Schofield of Cambridge University must be congratulated for revitalizing this technique as early as 1965. The number of papers presented in this session on the centrifuge clearly indicates potential use in the future on a worldwide basis.

From the foregoing discussions, I would like to recommend that:

- (i) there is an urgent need to standardize notations and terminology.
- (ii) concepts such as critical state, normality etc. are to be now taught at undergraduate levels in regular civil engineering programs,
- (iii) students at undergraduate level are also to be taught in statistical concepts and data analysis.
- (iv) future emphasis on research be directed on such materials as partially saturated soils, residual soils, dispersive soils, soft rocks, etc.
- (v) centrifugal model tests are to be included wherever possible in modelling full scale behaviour, where the expense and effort for carrying out full scale tests are substantially high.

Finally, standardization of laboratory tests must be encouraged wherever possible and more contributions are to be invited on the relevance of laboratory testing in future conferences.

tudes above 1 1/2% strain, with no drainage, hysteresis stress/strain diagrams are typically as shown in Fig. 1 (from Ref. 1). As the test progresses, the maximum stress decreases as a result of degradation. The loop develops the shape shown, with a double curvature, the tangent modulus increasing with increase in strain. (This does not occur at amplitudes below about 1%). The pore pressures vary cyclically with strain as shown in Fig. 2. The concept I wish to present, is that these pore pressure

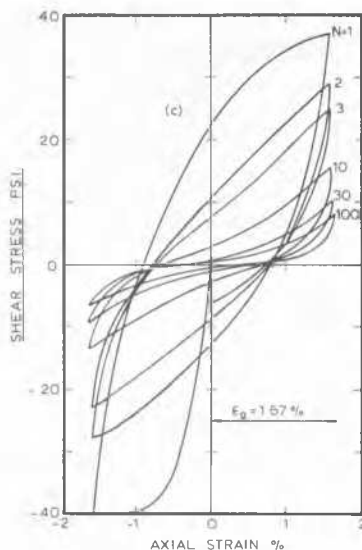


Fig. 1. Typical stress/strain diagrams.

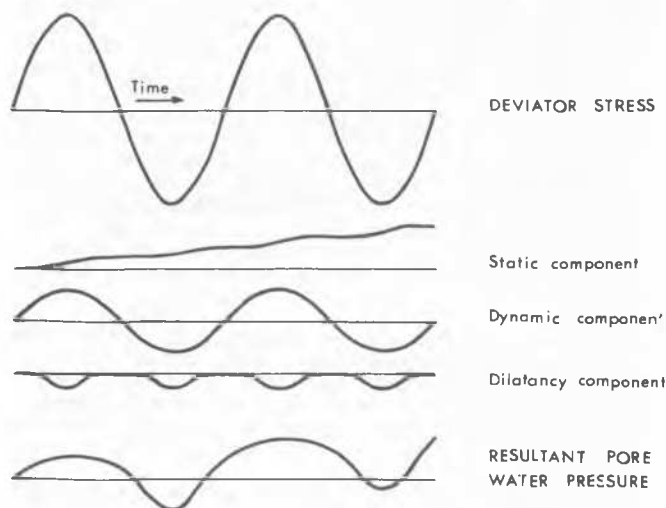


Fig. 2. Components of pore water pressure.

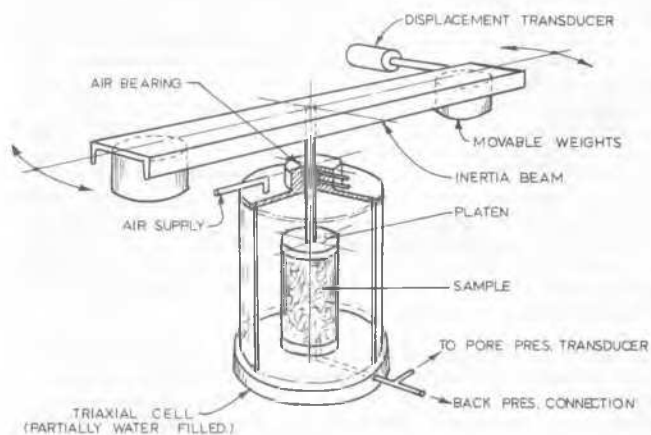


Fig. 3. Apparatus for free vibration torsion test.

changes can be subdivided into three components:

1. A static component which continually increases throughout the test and is a result of changes in soil microstructure. This component causes the degradation observed.
2. A dynamic component, proportional to the cyclic deviator stress. Our research has shown the amplitude to correspond to a value of Skempton's pore pressure parameter $A = \frac{1}{3}$. This is the theoretical value obtained for a purely elastic soil skeleton.
3. A dilatancy component which increases to a maximum negative value at peak strain (positive or negative) and accounts for the increase in tangent modulus.

The second point concerns the use of the free vibration torsion test. A form of this apparatus (first devised by Zeevaert in 1967), has been developed at the University of Auckland and was described in a paper to the Moscow conference (Ref. 2) and, more recently by Taylor and Larkin (Ref. 3) from which Fig. 3 is taken.

The sample acts as a torsion spring for the inertia mass connected to it through a universal joint. Friction is eliminated by the use of a pair of air bearings. The masses are such that the frequency is about 2 cycles/second, which is within the range for earthquakes. Its operation is very simple - a cam is used to provide the initial torsional deformation, of controlled magnitude and the free vibrations thereafter are recorded. By accurately measuring the frequency the shear modulus can be found, and from the decay of the vibrations, the equivalent viscous damping is obtained. Three tests of successively increasing initial amplitude, give the shear modulus over the range 1×10^{-6} to 0.5×10^{-2} (one microstrain to $1/2\%$).

While fairly elaborate recording apparatus is required to cover this range the test method is very much simpler than resonant column tests and, in my opinion, offers numerous other advantages. It is surprising, therefore, that the free vibration torsion test has not been more widely adopted.

The third and last point relates to the correlation of field and laboratory measurements. It is being increasingly recognised that, wherever possible, field measurements are to be preferred to laboratory tests. As one example of this, in the realm of soil dynamics, I refer to the determination of shear modulus. It is not possible (or if it is, then it is extremely difficult and expensive) to determine the shear modulus of a soil in the field at large amplitudes. It can readily be done, however, at low amplitudes by measurement of shear wave propagation velocity. The shear modulus so obtained can be compared with the laboratory value at a shear strain of 10^{-5} or less. Provided high quality sampling methods are used we have found, at Auckland, that the correlation is good for the cohesive soils we have tested when compared with shear wave velocity determinations using down-hole techniques.

References:

1. Taylor, P.W. and Bacchus, D.R., "Dynamic cyclic strain tests on a clay", Proc. 7. Int. Conf. Soil Mechs. and Found. Eng. (Mexico) Vol. I, p. 401 (1969).
2. Taylor, P.W. and Parton, I.M., "Dynamic torsion testing of soils", Proc. 8. Int. Conf. Soil Mechs. and Found. Eng. (Moscow) Vol. I, p. 425 (1973).
3. Taylor, P.W. and Larkin, T.J., "Seismic site response of non-linear soil media", Jour. Geotechnical Eng. Div., ASCE, Vol. 104, GT3, p.369.

INTRODUCTION

My contribution is concerned with the interpretation of laboratory tests and the use of stress-strain data in both understanding model tests, such as those carried out in the centrifuge, and also for design of geotechnical works. It is hardly necessary to point out the electronic and computing revolution that is being experienced, and the contrast between the early apparatus and techniques of soil mechanics 30 years ago, described by Professor Bishop in his special lecture, and the sophisticated equipment for soil testing displayed in GeoEx 81. It is now possible to conduct tests which are controlled by a computer to follow specially selected effective stress paths, with automatic recording of a large amount of data to a high degree of accuracy.

The question arises as to how accurate these data are, due to deficiencies in the apparatus itself and whether proper and rational allowance can be made for them. Because of (i) end-effects, (ii) friction between the sample and platens, and (iii) mixed boundary conditions (some being displacement controlled and some stress-controlled), non-uniformities develop within the sample. Observations made at the boundaries of the sample do not represent what is happening within the sample; this fact is of particular importance in cyclic testing, as is well recognised.

It is now possible to study the magnitude of these boundary effects by considering a single test as a boundary value problem itself, and carrying out a finite element computation in an attempt to simulate numerically the non-uniformities that may develop in the actual test. To illustrate this, I shall present the results of a series of finite element computations of the basic triaxial compression test on a normally consolidated remoulded clay. These calculations were carried out by Dr. J.P. Carter at the University of Cambridge in 1978 and they are reproduced with his kind permission; they are to be published by Carter (1982).

NUMERICAL MODELLING OF TRIAXIAL COMPRESSION TEST

An idealised triaxial test has been studied in which the end platens have been assumed to be perfectly rigid and frictionless. The platens provide displacement controlled boundaries, and the rubber membrane provides a stress controlled boundary. The sample has a filter drain around its cylindrical surface, so that free drainage is assumed to occur on all boundaries. The finite element mesh chosen to represent the sample is shown in Fig.1. Points A, B and C are the median points of three elements which experience very different stress paths on account of their different positions within the sample.

The purpose of the computations was to study the effects of carrying out the test at different strain rates, with the consequence that there are different degrees of drainage and of consolidation, and non-uniformities develop within the sample due to hydraulic effects.

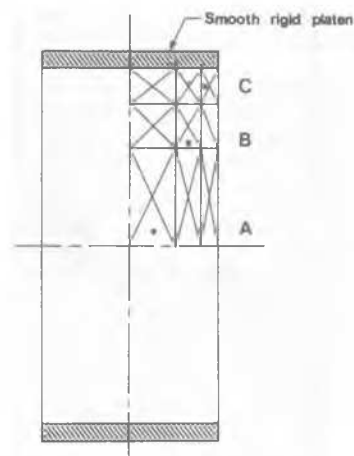


Fig.1 Finite Element Mesh for Triaxial Sample

In order to make the computations as realistic as possible and to allow a comparison to be made with published experimental data, it was decided to model the results of tests on normally consolidated remoulded Weald clay, reported by Bishop and Henkel (1962) and Gibson and Henkel (1954). The choice of mathematical model for representing the behaviour of the clay is critical in this case because of the large plastic strains that develop and the need to represent the stress-strain relationships in terms of effective stresses. The modified Cam-clay model was used, as it is particularly well-suited for modelling the behaviour of normally consolidated clay. It is also important to use an incremental analysis which incorporates a fully coupled Biot-type of consolidation.

The parameters for the soil model (including the coefficient of permeability) were chosen to match as closely as possible the data of conventional consolidation tests, and one fully drained triaxial compression test (curve No.1 in Fig.2): the full details are given by Carter (1982).

All five samples were simulated as being initially isotropically consolidated to a pressure of 30 lbf/in² (207 kN/m²) with an initial voids ratio of 0.630. The computed stress-strain curves are shown in Fig.2, where the deviator stress at the sample boundary (i.e. the total load on the platen divided by its area, less the cell pressure) is plotted against the overall axial strain (i.e. the total shortening of the sample divided by its initial length). The experimental curves are for a fully drained test and a fully undrained test, which compare very closely with the slowest and fastest rates of strain respectively (curves 1 and 5). The three intermediate curves (2, 3 and 4) are for the three quoted intermediate rates of strain, and illustrate clearly the consequences of a decreasing amount of drainage and consolidation, as the strain rate increases.

It should be emphasised that these curves are all based on the same set of soil properties; the only difference being the rate of strain. This is a special feature of the Cam-clay model,

which is not an integral part of most other mathematical models of soil behaviour.

The peak value of deviator stress for each of the computed curves is plotted in Fig.3 against the rate of axial strain, both for the case of drainage from all faces of the sample (as in Fig.2) and also for drainage from both ends only. The former can be compared very favourably with eight experimental results taken from Gibson and Henkel (1954).

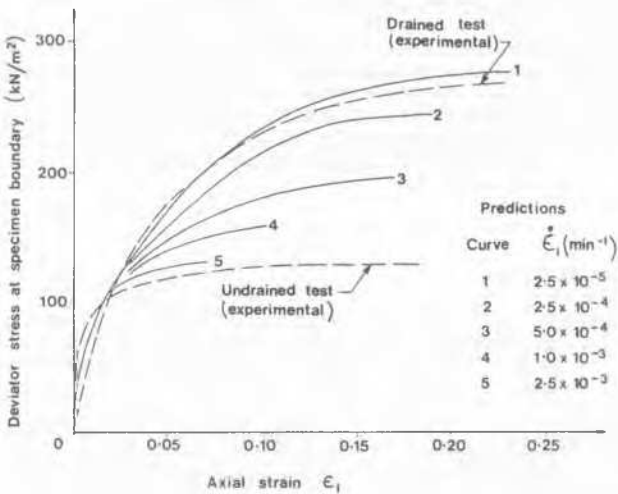


Fig.2 Stress-strain Curves for Different Rates of Strain

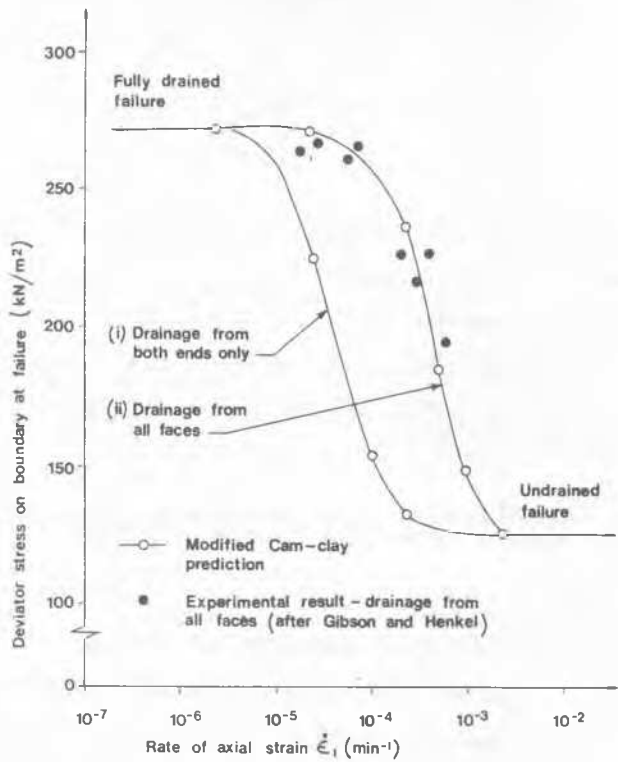


Fig.3 Variation of Strength with Axial Strain Rate

NON-HOMOGENEITY WITHIN A SAMPLE

The greatest degree of non-uniformity within the samples occurs for case 3 ($\dot{\epsilon}_1 = 5 \times 10^{-4} \text{ min}^{-1}$); this is illustrated in Fig.4 at the instant when the axial strain is 0.05, by means of contours of mean effective principal stress p' , deviator stress q , pore-pressure u and voids ratio e , in the respective quadrants.

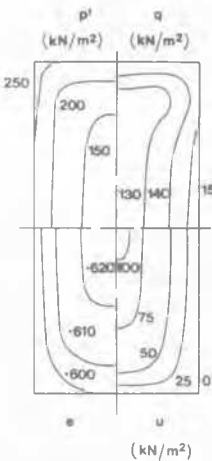


Fig.4 Contours of Stresses and Voids Ratio Within Sample ($\dot{\epsilon}_1 = 5 \times 10^{-4} \text{ min}^{-1}$; $\epsilon_1 = 0.05$)

An alternative way of presenting the severe degree of non-uniformity in the partially drained sample 3 (tested at the intermediate strain rate

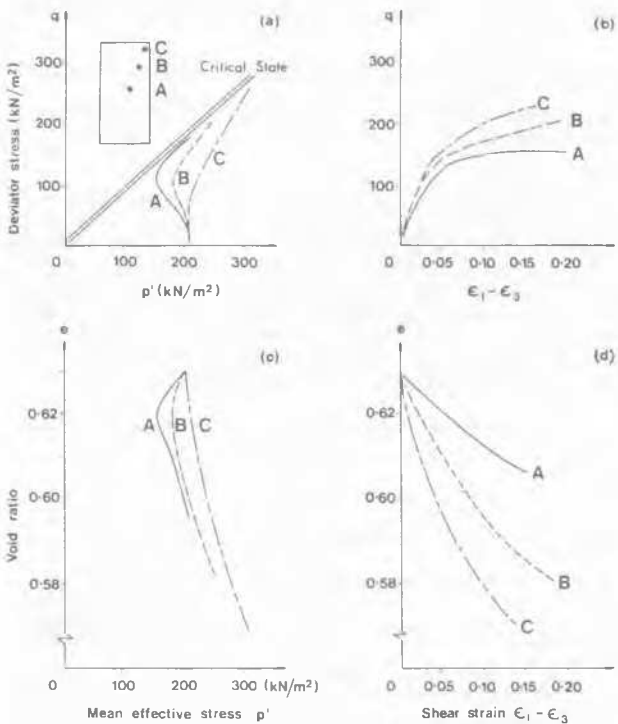


Fig.5 Test Paths Computed for Three Elements in a Sample ($\dot{\epsilon}_1 = 5 \times 10^{-4} \text{ min}^{-1}$)

of $\dot{\epsilon}_1 = 5 \times 10^{-4} \text{ min}^{-1}$) is by means of the individual paths for the separate elements A, B and C in Fig.5. This diagram shows four inter-related plots of the four variables p' , q , e and shear strain $\epsilon_1 - \epsilon_3$. It should be noted that element C close to the boundary where free drainage occurs behaves like a fully drained sample, whereas element A near the centre behaves initially like an undrained sample. Towards the end of the test, when sufficient time has elapsed for most of the excess pore pressures to have dissipated, the effective stress path for element A in Fig.5(a) turns back on itself and becomes tangential to the failure envelope formed by the critical state line.

CONCLUSIONS

I have presented some predictions of non-homogeneous behaviour in triaxial specimens of clay. Only those have been considered which arise due to the effects of a finite coefficient of permeability, a finite loading rate and migration of pore water within and from the specimen. The effect of rough end platens has not been included here, although this has been considered separately by Carter.

It has been shown that the modified Cam-clay soil model, when used together with a coupled Biot-type consolidation analysis in a finite element computation, can make reasonable predictions of the non-homogeneous behaviour of a sample of normally consolidated clay in a triaxial compression test.

There is a need, which can now be met, of carrying out numerical experiments in parallel

D.Y.F. Ho and D.G. Fredlund (Oral discussion)

Discussion on the paper "SHEAR STRENGTH OF PARTIALLY SATURATED SOILS" by S.K. Gulhati and B.S. Satija. (Vol. 1, p. 609)

The discussers would first like to compliment Professor Gulhati and Dr. Satija for completing a very demanding and excellent unsaturated soil testing program. The discussers, however, have some concern over the manner in which the test data was interpreted. Namely, the interpretation presented by the author's paper does not render a smooth transition between the conventional saturated soil shear strength equation (Terzaghi, 1936) and the proposed equation for unsaturated soils.

The saturated soils shear strength equation as per Terzaghi (1936) is as follows:

$$\tau = c' + (\sigma - u_w) \tan \phi' \quad (1)$$

where τ = shear strength of the soil

c' = effective cohesion

σ = total stress

u_w = pore-water pressure

ϕ' = effective angle of internal friction

In a stress point form, the equation reads;

with laboratory experiments in order to:

- (i) prove the success of computational techniques,
- (ii) check the relevance of mathematical models,
- (iii) indicate the extent of the deficiencies of apparatus, and
- (iv) understand and interpret the results of centrifugal model tests.

Such work has applications not just for research purposes, but is now being used for design of engineering works. One important example which has been successfully tackled is the problem of a road embankment built on soft ground and the possible need for staged construction to avoid stability problems.

REFERENCES

- Bishop, A.W. and Henkel, D.J. (1962). The measurement of soil properties in the tri-axial test, 2nd Ed., London:Edward Arnold Ltd.
- Carter, J.P. (1982). Some predictions of the non-homogeneous behaviour of clay in the triaxial test. Géotechnique (in press).
- Gibson, R.E. and Henkel, D.J. (1954). Influence of duration of tests at constant rate of strain on measured 'drained' strength. Géotechnique, 4, 6-15.

$$1/2(\sigma_1 - \sigma_3) = d' + [1/2(\sigma_1 + \sigma_3) - u_w] \tan \psi' \quad (2)$$

where σ_1 = major principal stress

σ_3 = minor principal stress

d' = the intercept when the stress point is zero

ψ' = the angle between the stress point plane and the

$[1/2(\sigma_1 + \sigma_3) - u_w]$ axis

The proposed equation for the shear strength of unsaturated soils presented in the paper is stated as follows:

$$\frac{(\sigma_1 - \sigma_3)}{2} \tau_f = a + (\sigma_3 - u_a)_f \tan \alpha + (u_a - u_w)_f \tan \beta \quad (3)$$

where σ_1 = total major principal stress at failure

σ_3 = total confining stress at failure

u_a = pore air pressure at failure

a = apparent intercept at the $(\sigma_1 - \sigma_3)$ axis of the three-dimensional plot between $(\sigma_3 - u_a)_f$ and

$$\left(\frac{\sigma_1 - \sigma_3}{2}\right)$$

α = coefficient with respect to changes in $(\sigma_3 - u_w)_f$ when $(u_a - u_w)$ is held constant

β = coefficient with respect to changes in $(u_a - u_w)_f$ when $(\sigma_3 - u_a)_f$ is held constant

The discussers would like to point out that the proposed equation for the shear strength of unsaturated soils is presented in a way which is neither in accordance with the Mohr-Coulomb failure hypothesis nor the stress point method (Figure 1). Moreover, there will not be a smooth transition between the proposed equation and Terzaghi's (1936) shear strength equation for saturated soils. When saturation is approached (i.e., $u_a = u_w$), the proposed equation does not revert back to Terzaghi's (1936) shear strength equation for saturated soils either in conventional or stress point form.

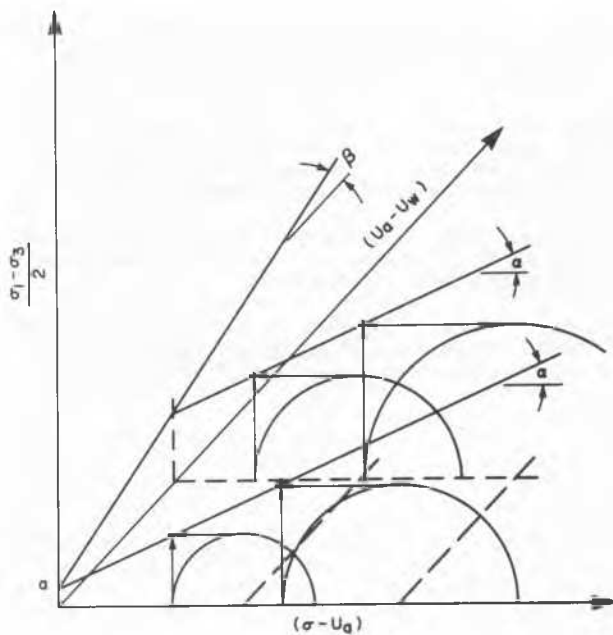


FIGURE 1 Satija's (1978) shear strength equation in three dimensional plot.

Fredlund et al (1978) have proposed shear strength equations for unsaturated soils utilizing the same independent stress state variables. When $(\sigma - u_a)$ and $(u_a - u_w)$ are used as the stress variables, the unsaturated soil shear strength equation as per Fredlund et al (1978) as as follows:

$$\tau = c' + (\sigma - u_a) \tan \phi' + (u_a - u_w) \tan \phi^b \quad (4)$$

where u_a = pore air pressure

ϕ^b = the friction angle with respect to changes in $(u_a - u_w)$ when $(\sigma - u_a)$ is held constant

In stress point form, the equation becomes,

$$1/2(\sigma_1 - \sigma_3) = d' + 1/2(\sigma_1 + \sigma_3) \tan \psi' + (u_a - u_w) \tan \psi^b \quad (5)$$

where σ_1 = the major principal stress (i.e., the total axial stress)

σ_3 = the minor principal stress (i.e., the total confining stress)

ψ^b = the angle between the stress point plane and the $(u_a - u_w)$ axis when $[1/2(\sigma_1 + \sigma_3) - u_a]$ is held constant.

Graphically, the failure envelope will be a planar surface in either conventional or stress point form (Figure 2 and 3). It should be noted that there is a smooth transition from Fredlund et al's (1978) unsaturated soil shear strength equations to the conventional shear strength equations for saturated soils (Terzaghi, 1936) As saturation is approached, the pore air pressure, u_a ,

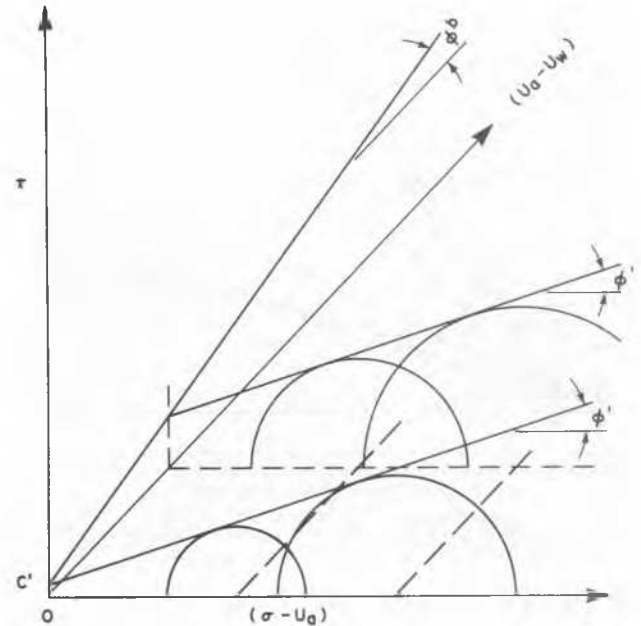


FIGURE 2 Three dimensional failure surface using stress variables $(\sigma - u_a)$ and $(u_a - u_w)$

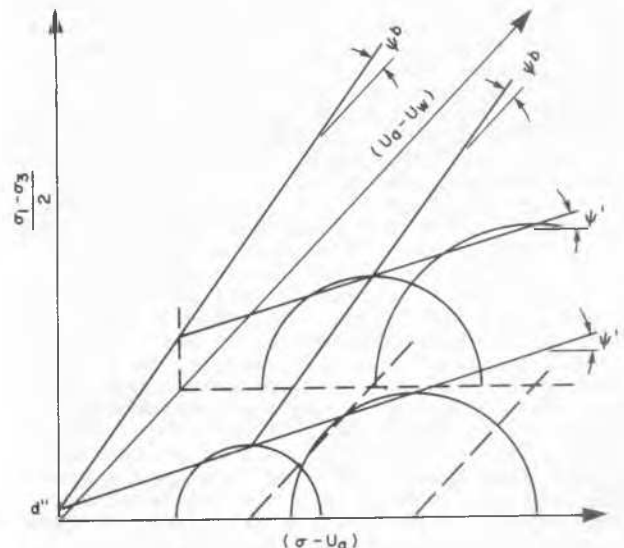


FIGURE 3 Fredlund et al (1978) three dimensional failure surface using stress variables $(\sigma - u_a)$ and $(u_a - u_w)$ in stress point form.

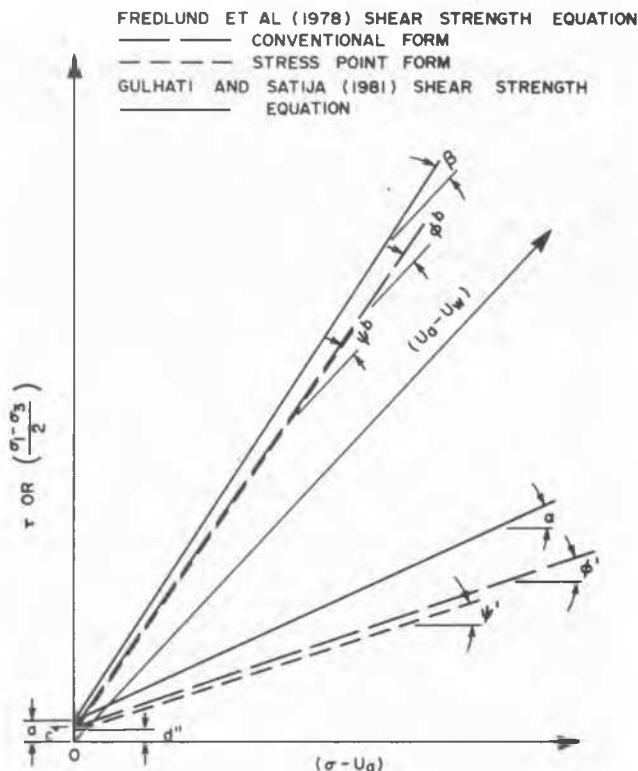


FIGURE 4 Comparison between unsaturated soil shear strength equations proposed by Fredlund et al (1978) and Satija (1978)

T. Kimura and K. Saitoh (Oral discussion)

ON THE COMPARISON OF CENTRIFUGE TESTS WITH LARGE-SCALE MODEL TESTS

In order to obtain practicable results through model tests simulating earth structures, it is essential that the law of similarity is maintained between the prototype and the model. For a problem in which the self-weight of soil is significant, conventional model tests do not allow us to model the prototype. One way of modelling this type of problem correctly is to use a centrifuge, and the usefulness of centrifuge modelling technique is now being widely recognized. It has to be pointed out, however, that the similarity law for centrifuge modelling is based upon the concept of continuum mechanics or the concept of stress in soil elements, not of soil particles. Some skepticism has been raised on this point, arguing that a slip band, in a model ground of sand for example, in a centrifugal field, say of Ng , would be N times wider than the actual one in the gravitational field leading to an unrealistic failure mode. But the Authors take a view that, as long as the same sand is used for a centrifuge test and a prototype, it would show a very similar behaviour since sand is essentially a frictional material.

In this short report the Authors attempt to put forward a comparison between centrifuge test results and those of large-scale model tests on

becomes equal to the pore water pressure, u_w . At this condition, Fredlund et al's (1978) unsaturated soil shear strength equations (equation 4 and 5) revert back to Terzaghi's conventional shear strength equations (equation 1 and 2) for saturated soils.

By comparing the unsaturated soil shear strength equations as per Fredlund et al (1978) with that presented by Gulhati and Satija (1981), it can be demonstrated that the proposed equation for the shear strength of unsaturated soils will predict too high a shear strength (Figure 4). In turn, the over-estimation of shear strength by Gulhati and Satija's equation would result in over-estimating factors of safety in slope stability analyses involving unsaturated soils (Ho, 1981).

While the discussers feel there is a superior procedure for interpreting the data of Gulhati and Satija, we want in no way to underestimate the value of the experimental test data.

List of References

- Fredlund, D. G., Morgenstern, N. R. and Widger, A., 1981. "Shear Strength of Unsaturated Soils", Canadian Geotechnical Journal, Vol. 15, No. 3, pp. 318-321.
- Gulhati, S. K. and Satija, D. J., 1981. "Shear Strength of Partially Saturated Soils", Proceedings of the Tenth International Conference on Soil Mechanics and Foundation Engineering, Stockholm, Sweden.
- Ho, D. Y. F., 1981. "The Shear Strength of Unsaturated Soils", M. Sc. Thesis, University of Saskatchewan, Saskatoon, Saskatchewan, Canada.
- Terzaghi, K., 1936. "The Shearing Resistance of Saturated Soils", Proceedings of the First International Conference on Soil Mechanics, Volume 1, pp. 54-56.

an identical problem of loaded slopes consisting of dense sand. Shields et al. (1977) performed a series of model tests on the bearing capacity of slopes of sand loaded on the top surface. The height of their slopes exceeded 2.0m, which was considered to be of the scale of actual slopes. Incidentally the Authors carried out very similar tests by using centrifuge to study the stability of tank pads underneath oil storage tanks.

A key sketch of the problem dealt with is given in Fig.1. The experiments were conducted for various combinations of four parameters; the breadth of a footing B , the height parameter β , the distance parameter λ and the angle of inclination of a slope α . The sand used was Toyoura sand, of which effective particle diameter was 0.13 mm and uniformity coefficient was 1.38. The sand was poured into a container from a hopper through two sieves to form sand deposit with

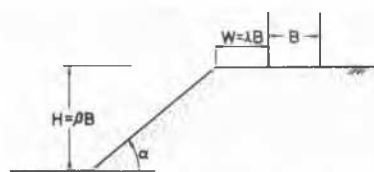


Fig.1 Key sketch of model

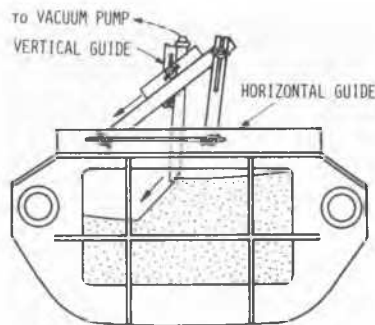


Fig.2 Slope former

uniform density. Subsequently a slope former shown in Fig.2 was assembled and attached to the container and the slope was formed by sucking in sand particles very carefully with a vacuum pump mounted on a guide frame. The relative density of completed slopes was approximately 90.0% with the

maximum variation of $\pm 1.5\%$. Plane strain shear tests were also conducted on Toyoura sand of the same lot after being consolidated in K_0 condition. The angle of shearing resistance ϕ was 49° under the mean effective normal stress of about 300 kN/m^2 , which was considered to be equivalent to the magnitude of the actual stress in slopes during centrifuge tests.

A radiograph for the case of $B=40 \text{ mm}$, $\beta=2$, $\lambda=0$ and $\alpha=30^\circ$ with the centrifugal acceleration of $30g$ is shown in Photo.1, in which well-developed failure lines can be observed. It is interesting to note that the angle between an oblique side of a wedge beneath the footing and the base is nearly equal to $\pi/4 + \phi/2$ but that the failure line of passive zone is fairly horizontal unlike the prediction based on the log-spiral method.

A relationship between the bearing capacity factor N_γ and the distance parameter λ obtained with centrifuge tests for $B=40 \text{ mm}$, $\beta=2$ and $\alpha=30^\circ$ under $30g$ is given in Fig.3. A solid line is a result reported by Shields et al. (1977) for silica sand with similar experimental conditions. Although the angle of shearing resistance of their sand is slightly larger than that of the Authors', the agreement between two results is rather remarkable.



Photo.1 Radiograph after failure ($\alpha=30^\circ, \beta=2, \lambda=0$)

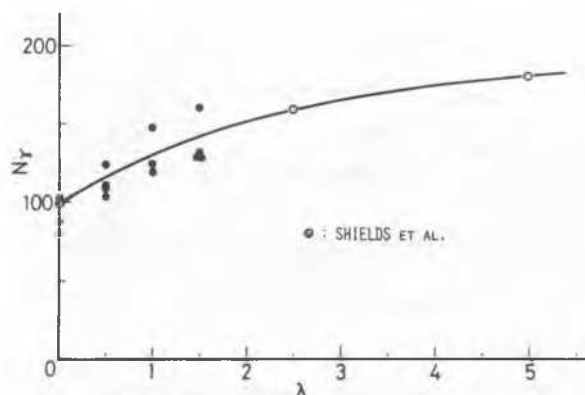


Fig.3 Relationship between bearing capacity factor N_γ and distance parameter λ

Reference

Shields, D.H. et al. (1977), "Bearing Capacity of Foundations Near Slopes", Proc. 9th ICSMFE Vol. 1, Tokyo

I.F. Symons (Oral discussion)

The Transport and Road Research Laboratory has carried out a programme of research with the aim of providing practical guidance for the design of buried flexible pipes, similar to that which exists in the UK for rigid pipes. The main components of the experimental work have involved full-scale studies on site and in the Laboratory's test pit (Trott and Stevens, 1979) together with static and centrifugal model tests carried out by the Engineering Group of Cambridge University (Valsangkar and Britto, 1978, 1979).

One series of tests has been carried out in which the behaviour of a full-scale pipe in the test pit was compared with that of a geometrically similar model tested in the centrifuge. The test pit is 5 m long by 3 m wide by 3 m deep and a 1 metre diameter steel pipe, 4.2 m in length and having a wall thickness of 6 mm was selected for these tests. The pipe was installed in dry sand compacted in 200 mm thick layers to give a depth of cover over the pipe crown of 250 mm. On completion of backfilling, surface loadings were applied over a 4.2 m long by 0.6 m wide strip placed along the pipe axis and also at offsets of 250 mm and 500 mm. The dimensions of the centrifugal model were selected to give similitude

with those of the full-scale pipe when tested at an acceleration of 9.2 gravities. To ensure uniform conditions around the model pipe the sand was placed by pouring parallel to the pipe axis.

The external strains measured after backfilling are shown in Figure 1. Only small strains were induced in the

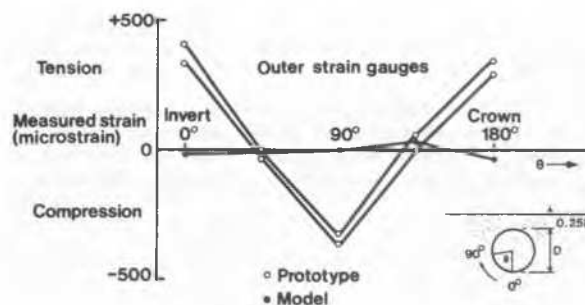


Fig. 1. Comparison of measured strains after backfilling

model pipe by the backfilling process and the diametral change was less than 0.25 per cent. By contrast the placement and compaction of the sand around the full-scale pipe induced much higher strains at the crown, invert and springing of the pipe together with an increase in vertical diameter of about 1.6 per cent.

The distribution of strain produced by the surface loading showed greater scatter from repeat tests on the full-scale pipe than on the model, although both showed the same pattern with large increases in strain confined to the upper segments of the pipes. This is illustrated in Figure 2 which gives the distribution of external strains produced by a central strip loading of 500 kN. For the full-scale pipe the strain distribution is quite different from that induced by back-filling with large increases in strain at the pipe shoulders and strain increments of opposite sign at the pipe crown.

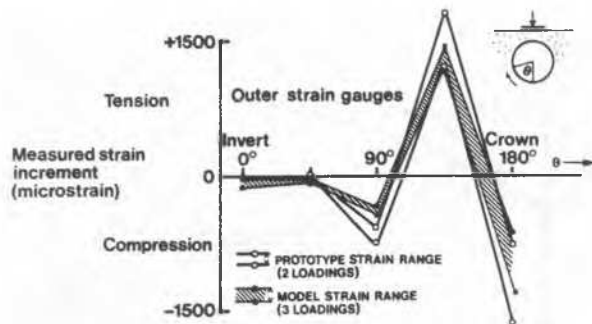


Fig. 2. Comparison of strain increments under central strip loading
- Total load 500 kN

In the final test of each series the model and prototype pipes were loaded to failure under a central strip loading. Failure occurred in the full-scale pipe at a total load of 520 kN and in the model at a scaled total load of 560 kN. The difference in these loads is close to the limit imposed by the accuracy in determining centrifugal acceleration. The mode of failure for the full-scale and model pipes was very similar and took the form of buckling at the pipe crown as shown in Figures 3 and 4.

The results therefore indicated that although differences in the method of placement of sand around the full-scale and model pipes were reflected in the strain and deflection pattern on completion of back-filling, generally good agreement was obtained in subsequent tests under the action of applied surface loadings.

REFERENCES

Trott, J. J. and Stevens, J.B. (1979) Loading tests on uPVC pipes installed in cohesive and non-cohesive bedding materials. Proc.4th Int.Conf. Plastic Pipes. University of Sussex, England.

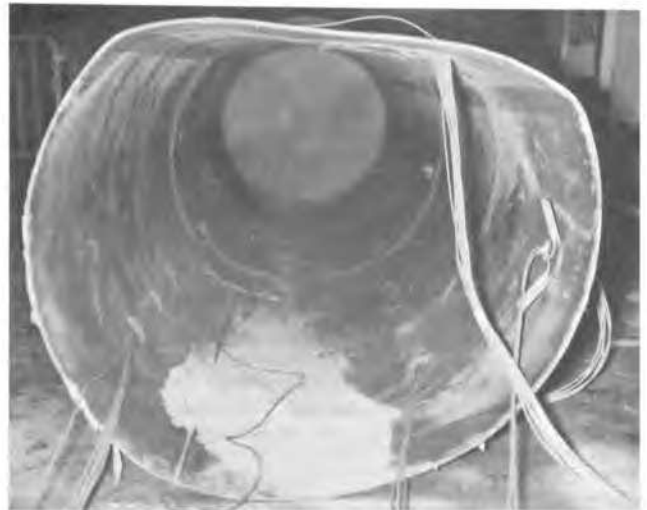


Fig. 3. Full-scale pipe after failure

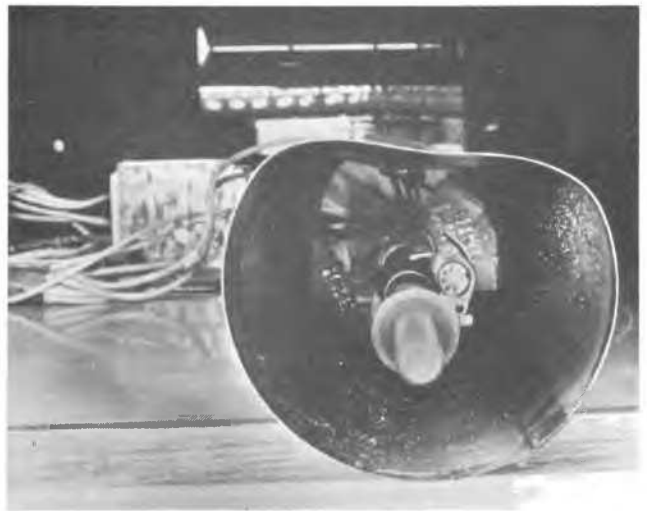


Fig. 4. Model pipe after failure

Valsangkar, A.J. and Britto A.M. (1978) The validity of ring compression theory in the design of flexible buried pipes. Department of the Environment Department of Transport, TRRL Report SR 440. Crowthorne, England (Transport and Road Research Laboratory).

Valsangkar, A.J. and Britto A.M. (1979) Centrifuge tests of flexible circular pipes subjected to surface loading. Department of the Environment Department of Transport, TRRL Report SR 530. Crowthorne, England (Transport and Road Research Laboratory).

D. Deveaux (Written discussion)

A PROPOS DE L'ESSAI DE CONSOLIDATION

Parmi les essais de Mécanique des Sols, l'essai oedométrique est de ceux qui fournissent les résultats les moins précis. Cette mauvaise qualité de prévision a été confirmée par les études de remblais en vraie grandeur, sur sols mous, surtout dans le cas de l'étude de la durée des tassements (Peignaud 1973, Magnan 1980). Les nombreuses études effectuées sur l'essai oedométrique ont montré l'importance du remaniement du matériau, des sollicitations parasites (frottement, centrage, chocs) et de la représentativité des échantillons. Les résultats expérimentaux que nous présentons ci-dessous conduisent à poser le problème du choix des hypothèses qui sont à la base du processus expérimental et de leur adaptation au fonctionnement du phénomène étudié. Les essais ont été effectués sur une cellule oedométrique avec mesure de pression interstitielle développée dans notre Laboratoire.

I - MATERIEL EXPERIMENTAL

La cellule d'essai intégrée comporte le vérin de mise en charge et les capteurs. L'échantillon de diamètre 7cm et d'éclatement 0.17 est drainé sur la face supérieure dans une chambre de contre-pression et la mesure de pression interstitielle est réalisée à la base. Le chargement de l'échantillon est effectué, soit en contraintes imposées (à l'aide d'un vérin pneumatique intégré), soit en déformations imposées. Lors de la conception et de la réalisation, une grande attention a été apportée à la recherche de la qualité des sollicitations et de la précision des mesures :

Type de capteur	Plage de mesure	Précision (EMQ)
déformation axiale	5 mm	2,5 µm
effort axial	500 daN	1 daN
pression interstitielle	300 kPa	0,3 kPa
Temps de réponse du vérin à un incrément de pression < 0,2 s		
Temps de réponse de la mesure de pression interstitielle 10 à 20 s		

L'acquisition des données et le contrôle de l'essai sont réalisés automatiquement à l'aide d'un mini-calculateur DEC PDP 11. Les logiciels de contrôle permettent la réalisation de nombreux types d'essais : essais standards à paliers, C.G. Test, C.R.S. Test et d'autres plus complexes dont l'étude est en cours.

II - PRESENTATION ET ANALYSE DES RESULTATS D'ESSAIS

Une dizaine d'essais de chargement par paliers a été réalisée à l'aide du matériel décrit ci-dessus sur des échantillons non remaniés ou reconstitués de trois types d'argiles : - argile minérale plastique : $w=60$, $I=30$, $w_L=40$ à 50 ; - argile molle faiblement organique : $w=125$, $I=80$, $w_L=113$; - argile tourbeuse : $w=145$, $I=90$, $w_L=125$. L'ensemble des essais représente environ une centaine de cas de charge, pour lesquels nous avons enregistré l'évolution de la déformation verticale (Δh) et de l'incrément de pression interstitielle à la base de l'échantillon (Δu_b), en fonction du temps. Malgré de petites différences liées au type d'argile et au mode de préparation des échantillons, le comportement observé est globalement le même pour les trois types d'argiles étudiés. Il fait apparaître notamment une décroissance de la pression interstitielle à la base plus rapide que le développement de la déformation. Cette observation semble indiquer que la déformation est retardée par rapport à l'application de la contrainte effective.

Cette déformation retardée est bien mise en évidence par la représentation de la figure 1 : ce diagramme traduit

l'évolution du rapport $(\Delta\sigma' - \Delta u_b)/\Delta\sigma'$ en fonction du degré de consolidation calculé à partir des déformations ($U_{def} = \Delta h_t/\Delta h_{100}$).

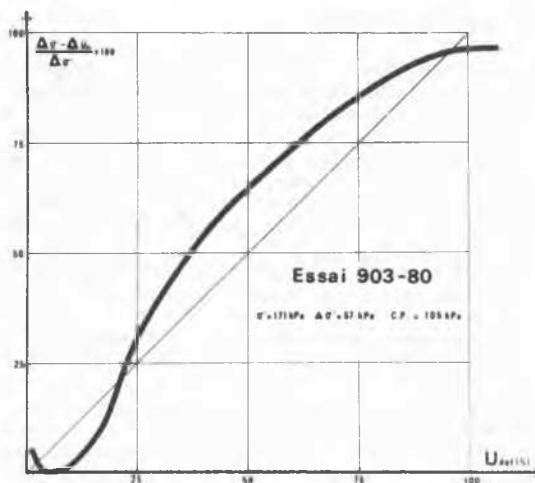


Figure 1

Pour un matériau qui ne présente pas de gonflement (ce qui est le cas des échantillons testés, qu'on a laissé librement se mettre en équilibre sous la contre-pression pendant au moins 48 heures), il est aisé de montrer que le rapport $(\Delta\sigma' - \Delta u_b)/\Delta\sigma'$ et le degré de consolidation U_{def} calculé à partir de la distribution de la pression interstitielle sont liés par la relation :

$$\frac{\Delta\sigma' - \Delta u_b}{\Delta\sigma'} < U_{def} \quad (1)$$

Le calcul du coefficient de consolidation C_v , à partir des courbes de déformation en fonction du temps est fondé sur l'hypothèse d'équivalence entre les deux degrés de consolidation ($U = U_{def}$). Si cette hypothèse était vérifiée les points expérimentaux devraient se situer dans le domaine situé sous la première bissectrice du diagramme de la figure 1 (d'après (1)). Or, les points expérimentaux se situent très vite en dehors de ce domaine, en traduisant une décroissance de pression interstitielle beaucoup plus rapide que prévu.

Afin de quantifier cette différence, nous avons calculé les coefficients C_v pour toutes les courbes situées dans le domaine normalement consolidé, ceci de deux manières différentes : - à partir des courbes de déformation par les méthodes de Taylor et Casagrande ($|C_v|_{def}$) ; - à partir des courbes d'évolution de pression interstitielle à la base : pour $U_{def} = 50\%$, $\Delta u_b/\Delta\sigma' = 78,2\%$ ($|C_v|_{u}$).

La comparaison entre les résultats obtenus peut être exprimée par le rapport suivant : $|C_v|_{u} / |C_v|_{def} = 5 \text{ à } 15$.

Ce rapport est peut-être à rapprocher de celui qui est observé quand on compare les comportements d'ouvrages "in situ" aux prévisions à partir des essais de laboratoire (Peignaud 1973, Magnan et Bagheri 1980).

$$\frac{|C_v|_{in situ}}{|C_v|_{essai}} = 10 \text{ à } 50$$

S. Leroueil (Oral discussion)

Interesting comments concerning the oedometer test have been made during the panel discussion by Professors Sällfors and Olson and the objective of this discussion is to emphasize some of them on the basis of experimental evidences gathered in Eastern Canada.

An extensive study on the preconsolidation pressure of sensitive clays has been performed these last two years on 8 sites underlain by Champlain sea clays. (Samson et al. 1981). On each site, the clay has been sampled with a 76 mm diameter piston sampler (area ratio 11%) and at one or two depths a series of oedometer tests were carried out. Constant rate of strain tests (CRS) using different rates, controlled gradient tests (CGT) using different gradients and usual step-loading tests with a load increment ratio of 0,5 and with each load maintained until the end of primary consolidation or for 24 hours depending on the tests.

All tests were performed in the same oedometer cell, specifically designed for that purpose.

The strong strain rate dependence of the deformation behaviour of sensitive clays already evidenced by Crawford (1965), Sällfors (1975) or Tavenas & Leroueil (1977) was confirmed and more precisely defined. In particular, when the preconsolidation pressure obtained from the tests is plotted as a function of the strain rate in CRS tests or of the strain rate at the preconsolidation pressure in CGT tests, or of the strain rate of the sample at the end of the loading periods for the 2 or 3 steps just following the preconsolidation pressure in step loading tests, it appears that there is a unique relationship between the preconsolidation pressure and the strain rate. Fig.1 shows such a relationship obtained for the Gloucester clay (Bozozuk & Leonards 1972).

Now, the question for an engineer is to know what the in situ preconsolidation pressure prevailing under an embankment will be? Which laboratory test will give the right answer? From the laboratory results previously mentioned it appears that the selection of the in situ preconsolidation pressure must be controlled by the strain rates in the clay foundations. However, the behaviour of the soil, and particularly the preconsolidation pressure observed in laboratory are also functions of the sampling technique used, of the storage conditions and of the testing method and equipment. So there is absolutely no a priori reason why a given laboratory test should give the correct in situ preconsolidation pressure. Therefore the only reasonable approach is to develop, on a regional basis, empirical correlations between in situ and laboratory preconsolidation pressures.

$$\sigma_p^i \text{ in situ} = f \times \sigma_p^i \text{ lab}$$

On 6 of the 8 sites studied by Samson et al. (1981), the

J. Biarez, P.Y. Hicher and C. Voyiatzoglou (Written disc.)

TROIS DOMAINES DE CHARGEMENT EN FATIGUE ET FLUAGE NON DRAINÉS POUR DES ARGILES SATURÉES

L'essai consiste à effectuer un chargement cyclique non drainé en augmentant la contrainte cyclique par paliers successifs. Le nombre de cycles par paliers est constant ainsi que l'incrément de contrainte d'un palier à l'autre. Nous présentons ici des résultats d'essais répétés ($0 \rightarrow q_c$) par paliers de 100 cycles sur des argiles saturées remaniées. Le paramètre représentant la fatigue du matériau est $a = \frac{\sigma_{100} - \sigma_{50}}{\log 100 - \log 50}$ et ϵ_{100} et ϵ_{50} représentant respectivement

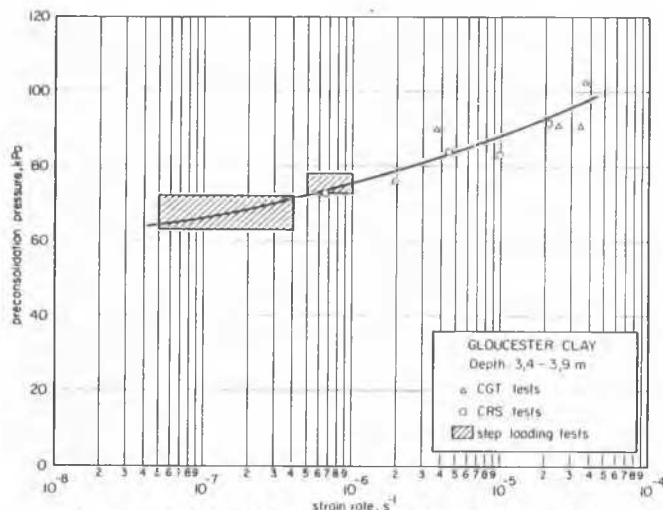


Fig. 1. Strain rate effect on the preconsolidation pressure

in situ preconsolidation pressure prevailing under loadings could be determined. It has been found that, for Champlain sea clays, when testing specimen obtained with a 76 mm diameter piston sampler, the usual oedometer test with a 0.5 load increment ratio and 24 hours maintained loads gives a preconsolidation pressure approximately equal to the in situ preconsolidation pressure ($f = 1,0$). On the other hand, the CRS tests and CGT tests performed at rates or gradients generally used, overestimate the in situ preconsolidation pressure and a correction factor is thus required. For a strain rate equal to $0,02\%/mn$ ($3,3 \times 10^{-6} s^{-1}$) this correction factor is approximately equal to 0,8.

References

- Bozozuk, M., Leonards, G.A. (1972). The Gloucester test fill. ASCE Specialty Conf. on Performance of Earth Supported Structures, Purdue, Vol.I, Part I, pp.299-317.
- Crawford, C.B. (1965). The resistance of soil structure to consolidation. Canadian Geotechnical Journal, Vol.2(2), pp.90-97.
- Sällfors, G. (1975). Preconsolidation pressure of soft high plastic clays. Ph.D. thesis, Chalmers University, Göteborg, Sweden.
- Samson, L., Leroueil, S., Morin, P., Le Bihan, J.P. (1981). La pression de préconsolidation des argiles sensibles. Report Terratech Ltd. No.1387-0 prepared for the National Research Council of Canada. 800 p.
- Tavenas, F., Leroueil, S. (1977). Effects of stresses and time on yielding of clays. Proc. 9th ICSMFE, Tokyo, Vol. 1, pp.319-326.

la déformation irréversible au 100^e et 50^e cycle. La figure 1 montre la variation de a en fonction du niveau de contrainte cyclique. Nous voyons que les courbes obtenues présentent deux coudes mettant en évidence trois régimes de fatigue.

Le premier régime est caractérisé par des valeurs très faibles de a . Cela veut dire que si le déviateur cyclique est inférieur à q_{c0} , valeur limite du premier domaine, la dé-

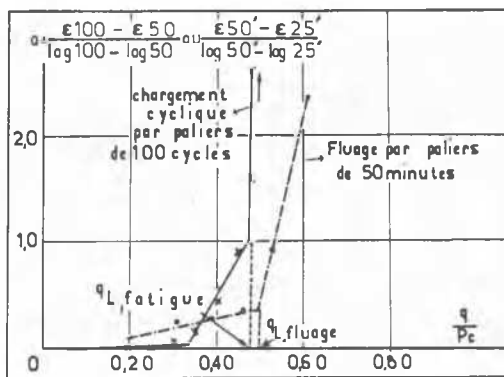


Figure 1 : Essais cyclique et de fluage par paliers sur l'argile noire ($P_c = 200$ kPa)

formation irréversible due à la succession des cycles sera faible et qu'il y aura stabilisation rapide du cycle contrainte-déformation.

Le deuxième régime montre une évolution quasi-linéaire de a avec la contrainte cyclique. Ici les déformations irréversibles peuvent prendre des valeurs importantes, parfois incompatibles avec la sécurité de la structure. Cependant le taux de déformation irréversible diminue de façon continue avec le nombre de cycles ce qui va conduire à une stabilisation du cycle contrainte-déformation pour un grand nombre de cycles (> 1000).

Pour des contraintes cycliques supérieures nous aurons rupture du matériau en régime cyclique. C'est ce qui caractérise le 3ème domaine où nous obtenons une brusque variation de a vers des valeurs très grandes. Ceci exprime une rapide détérioration du matériau pouvant mener jusqu'à la rupture si l'essai est poursuivi pendant un nombre de cycles suffisant.

Nous avons comparé les valeurs de q_{cL} avec celles obtenues par la méthode de la droite de stabilisation décrite par différents auteurs : Hicher (1979), Sangrey (1969), Voyiatzoglou (1980). (Figure 2). Nous obtenons une très bonne concordance. L'intérêt de la méthode que nous présentons ici est qu'elle ne nécessite qu'un seul essai alors qu'avec la méthode en contraintes effectives il faut au minimum 3 à 4 essais pour avoir la précision suf-

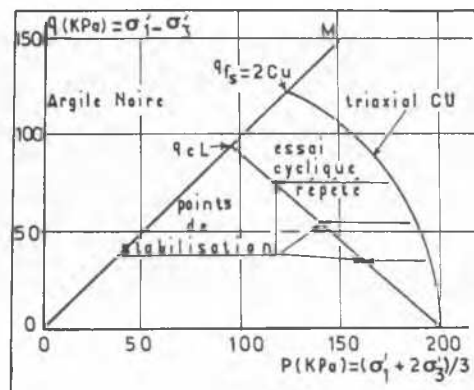


Figure 2 : Essais cycliques répétés sur l'argile noire ($P_c = 200$ kPa)

fisante sur la détermination de la droite de stabilisation. Le comportement original décrit par 3 domaines distincts n'est pas propre aux essais cycliques. Ainsi nous avons réalisé des essais de fluage non drainés avec la même procédure et nous retrouvons le même type de résultats (figure 1). Nous voyons de plus que la contrainte limite de fluage est proche de la contrainte cyclique limite pour des sollicitations de type répété.

De même différents essais in-situ faisant appel à une méthodologie comparable donnent des résultats qualitatifs identiques : c'est le cas des essais pressiométriques, des essais d'arrachement de pieux ou des essais de tirants d'ancrage. Des essais pressiométriques cycliques par paliers réalisés en Mer du Nord ont donné des résultats prometteurs qui sont présentés par Mizikos (1980).

BIBLIOGRAPHIE :

Hicher, P.Y. : (1979) Contribution à l'étude de la fatigue des argiles - Thèse de D.I. - Ecole Centrale de Paris - Mizikos J.P et Leroy J.P : (1980) Realities concerning cyclic loading a clay below a gravity structure. Europec Sangrey, Henkel, Esrig : (1969) The effective stress response of a saturated clay to repeated loading. Canadian Geotechnical Journal. Voyiatzoglou C : (1980) Contribution à l'étude de la fatigue et du fluage des argiles. Thèse de D.I. - Ecole Centrale de Paris -

G.T. Houlsby (Written discussion)

THE SHEAR STRENGTH OF A SOIL AT THE LIQUID LIMIT La Cohésion du Sol à la Limite de Liquidité

SYNOPSIS

The fall cone Liquid Limit test is interpreted theoretically as a strength test and the theory is in reasonable agreement with empirical correlations. The effect of cone roughness is important.

INTRODUCTION

The fall cone test is now widely used to establish the Liquid Limit, and is preferred to the Casagrande method in the British Standard. The test is essentially a simple strength test, and the depth of penetration h in Fig.1 depends on the weight of the cone Q , the shear strength of the soil c_u , the cone angle (which is 30° for the British Standard device) and the cone roughness.

For the Liquid Limit test the depth and weight are fixed, so that the test determines a particular

strength. Empirical correlations for the strength at the Liquid Limit exist, and the purpose of this discussion is to compare a theoretical calculation with these correlations.

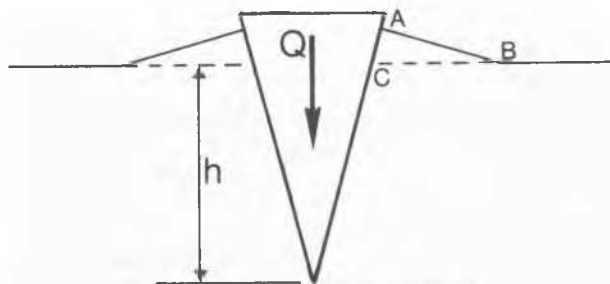


Fig.1 The Fall Cone Test

ANALYSIS

The analysis of the fall cone test uses the lower bound theorem of plasticity theory, with the approach being similar to the use of the method of characteristics in plane strain, but with the governing equations changed to those of axis-symmetry. As the cone penetrates the soil surface, a deformed zone ABC in Fig.1 is formed. The effect of this is accounted for approximately in the calculation (Houlsby, 1981). The dynamic effects of the fact that the cone is dropped rather than slowly lowered are accounted for, and it can be shown that the effects of soil density are negligible.

RESULTS

The results are presented in Table I in terms of a dimensionless factor $Q/c_u h^2$ for the 30° fall cone. The theory shows that the cone resistance depends strongly on the fraction of the undrained shear strength a/c_u mobilised at the surface of the cone, i.e. the cone roughness. Clearly this should be specified for a properly standardised test.

Wroth and Wood (1978) give a shear strength of 1.7 kPa for the British Standard cone (80 g with 20 mm penetration) from the results of many experiments. Piaskowski (1981) gives 5 kPa for a different device (100 g with 14 mm penetration). These give $Q/c_u h^2$ values of 1.15 and 1.04 respectively, and Karlsson (1961) gives results indicating a value of 1.25 for the 30° cone. These are all rather higher than the theory indicates, so that the theory overestimates the strength at

W.X. Huang, J.L. Pu and Y.S. Sun (Written discussion)

DISCUSSION ON CONSTITUTIVE RELATIONS

In response to the suggestion made by Messrs. P.V. Soos and G. Sällfors in their General Report of Session 4, we would like to make the following supplement to the paper presented by the writers (Huang et al, 1981) to this conference.

In order to investigate the influence of stress path on the shape of the equipotential surface, triaxial compression tests with the octahedral normal stress $p = \text{constant}$, i.e. $p = 200, 400$, and 600 kPa were performed besides the results of the $\sigma_3 = \text{constant}$ tests reported in the paper. Fig.1 shows the $q - \epsilon_a$ and $\epsilon_a - \epsilon_v$ curves obtained for $p = 400$ kPa, wherein ϵ_a and ϵ_v denote the total axial strain and volumetric strain respectively.

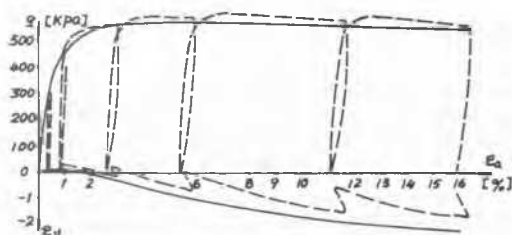


Fig. 1

The octahedral plastic shear and volumetric strains at points A and B (Fig.3) which are the intersection of two stress paths ($\sigma_3 = \text{const}$ and

TABLE I

Effect of Roughness on Cone Resistance

a/c_u	$Q/c_u h^2$
0.0	0.375
0.2	0.452
0.4	0.526
0.6	0.596
0.8	0.656
1.0	0.714

the Liquid Limit; the difference is, however, not unreasonable.

REFERENCES

- Houlsby, G.T. (1981). Theoretical analysis of the fall cone test. OUEL Report No. 1360/81, University of Oxford, Dept. of Engineering Science.
- Karlsson, R. (1961). Suggested improvements in the Liquid Limit test, with reference to the flow properties of remoulded clays. Proc. 8th Int. Conf. Soil Mech. Found. Engg, (1), 171-184, Paris.
- Piaskowski, A.M. (1981). An attempt of a new classification of cohesive soils. Proc. 10th Int. Conf. Soil Mech. Found. Engg, (1), 737-740, Stockholm.
- Wroth, C.P. and Wood, D.M. (1978). The correlation of index properties with some basic engineering properties of soils. Can. Geotech. J., (15), 137-145.

$p = \text{const}$) in $p-q$ plane as determined from the two different sets of test are shown in Table I.

TABLE I

point	$\bar{\epsilon}^p$ (%)		$\bar{\epsilon}_v^p$ (%)	
	$\sigma_3 = c$	$p = c$	$\sigma_3 = c$	$p = c$
A	0.155	0.150	0.58	0.57
B	0.097	0.083	0.71	0.72

From this table it can be seen that the octahedral plastic shear and volumetric strains at points A and B for $p = \text{const}$ tests and $\sigma_3 = \text{const}$ tests are approximately equal.

The plastic strain increment vectors at points A and B are shown in Fig.2 for the two different sets of test. The equipotential loci in the $p-q$ plane obtained directly from the tests are shown in Fig.3.

It may be seen from Fig.2 and Fig.3 that the plastic strain increment vectors and the equipotential loci for the two different stress paths are close to each other.

Comparison between the experimental data and the calculated stress-strain relation for $p = \text{const}$ stress path using parameters obtained from $\sigma_3 = \text{const}$ test is given in Fig.4. The agreement is found to be satisfactory.

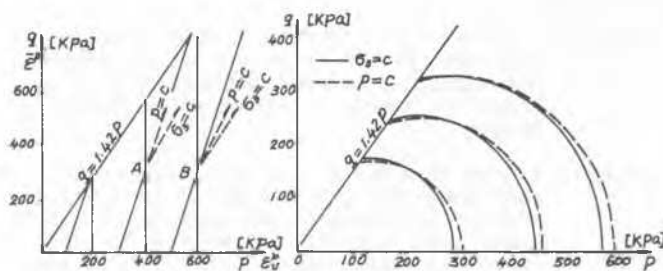


Fig. 2

Fig. 3

From the results thus obtained it may be concluded that for the medium Chengde sand studied the effect of the stress path on the parameters of the elasto-plastic matrix $[D]_{ep}$ is negligible if the stress path in the p - q plane is in the range between $\sigma_3 = \text{const}$ and $p = \text{const}$.

B. Kamenov and Z. Kysela (Written discussion)

CYCLIC LOADING OF SAND

/Written discussion to the contribution No. 4/23 Wen-Xi Huang, Jia-Liu Pu, Yu-Jiong Chen: "Hardening Rule and Yield Function for Soils", Vol.1, p. 631/.

According to the paper No. 4/23 the elastic shear modulus G depends on the state of stress of the soil and atmospheric pressure. In this respect we consider it desirable to present some results of research carried out by the authors of this discussion in the field of cyclic loading of sand /compare Fig.2 in Paper No. 4/23/.

The subject of investigation were the manifestations of fatigue and consolidation of soils under repeated shear loading. The tests were carried out in the shear box apparatus. The apparatus of proprietary design recorded continuously the dependence of the shear stress τ on the displacement Δl of the shear box with controlled changes of the shear stress. Major number of tests were carried out by the authors of this discussion with passing loading/periodical change of τ to zero while $\sigma_n = \text{const.}$ / with selected differences $\Delta l_{i+1} - \Delta l_i$ at the beginning of every τ reducing cycle.

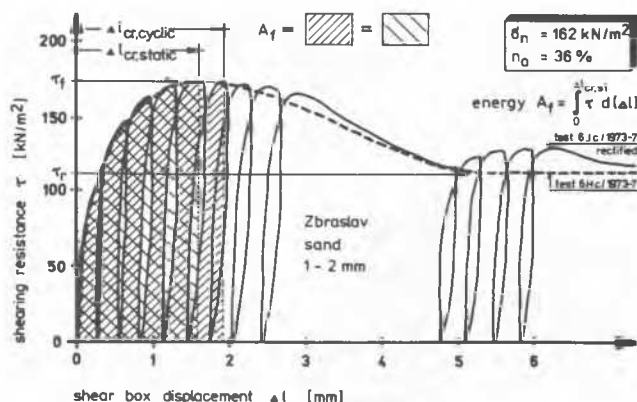


Fig.1. Diagram of the static and cyclic shear box test.

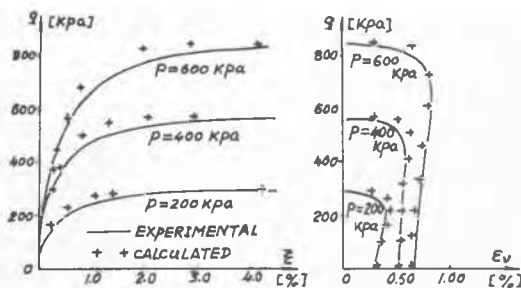


Fig. 4

REFERENCE

Wen-Xi Huang et al., (1981). Hardening Rule and Yield Function for Soils, Proceedings of X ICSMFE. Vol.I, pp 631-634.

In all cases there appeared a dependence of the shape and inclination of the passing shear stress loops on the preceding testing process.

The tangent to the declining branch of the loop is characterized in every point by the instantaneous elastic shear modulus \bar{G} . The mean value of G for one reduction of τ depends also on deformation work corresponding with equal displacement Δl in a static test, on the energy ΣW represented by the area of hysteresis loops, on the changes of structure and other factors. Most important are probably the changes of the soil structure produced or accelerated by the effect of energy induced into the soil by every loading cycle. These changes of structure depend on the number of preceding cycles. The loops of passing shear stress usually have different areas and inclinations depending on the ratio of the preceding shear stress τ to the peak strength τ_f , on the displacement Δl before the relief of τ , on the ratio of $\Delta l / \Delta l_{crit}$ [Δl_{crit} being the displacement at which τ_f has been attained], on the vertical stress of the sample, on initial porosity, on the course of changes of τ and on the number of relief cycles.

It has been shown that τ_f is attained with the displacements of $\Delta l_{cr,static} \ll \Delta l_{cr,cyclic}$.

If the number of cycles is small, the soil fatigue can be neglected for medium to heavily consolidated sands. In that case the equality of energies holds, shown in Fig. 1 by different types of hatching. A major number of cycles in a similar test has not resulted in the attainment of τ_f due to the soil fatigue. Furthermore, Fig. 1 shows that τ becomes stable at the residual value of τ_r like in the static test, after the cyclic loading has been interrupted. The renewed introduction of cyclic loading results in an increase of the shear

strength of the soil, the energy W represented by the loop being several times higher than that corresponding with similar τ at the beginning of the test.

For the description of the changes of the shear strength in dependence on its partial or complete repeated relieving the energy method suggested previously /Kamenov, 1962/ and further developed /Kamenov and Kysela, 1977, 1979; Kysela and Fíft, 1974/ subsequently seems promising. The strength and strain characteristics of the soil under variable load depend on the amount of energy induced into the soil and on the changes of soil structure. In simple cases it is possible to use the energy calculation to foresee the strength and strain soil characteristics after a certain period of application of variable load. The exhausting of shear strength of the soil after several dozens of loading cycles or the change of G to 50 - 500% after 7 - 10 cycles for the displacements of $\Delta l \ll \Delta l_{cr}$

H. Matsuoka (Written discussion)

PREDICTION OF PLANE STRAIN STRENGTH FOR SOILS FROM TRIAXIAL COMPRESSION

The "Spatial Mobilized Plane(SMP)" is such a plane that three two-dimensional sliding ("mobilized") planes between the respective two principal stress directions(I-II, II-III and I-III) are the three sides as shown in Fig.1($\tan(45^\circ + \phi_{moij}/2) = \sqrt{\sigma_i/\sigma_j}$; $i, j=1, 2, 3$, $i < j$), and is considered to be the plane where soil particles are most mobilized on the average under the three-dimensional stress conditions. The SMP provides a unique interpretation of the stress-strain behaviour up to the failure criterion under a general stress system. It offers advantages over criteria based on the stresses on the octahedral plane, which currently receive popularity.

The following failure criterion for soils has been proposed on the assumption that soils fail when the shear-normal stress ratio on the SMP τ_{SMP}/σ_{SMP} reaches a limiting value(Matsuoka and Nakai, 1974, 1977; Matsuoka, 1976).

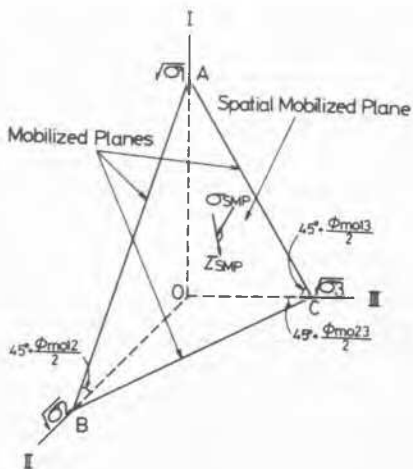


Fig.1 Spatial Mobilized Plane (ABC)

are not exceptional.

REFERENCES

- Kamenov, B. /1962/. State of stress, strain and strength of loose soils. /Napjatost, přetváření a pevnost sybkých zemin./ Internal Research Report, UTAM ČSAV, Prague.
- Kamenov, B. and Kysela, Z. /1977/. Subbase soil properties with regard to dynamic effects on building structures. /Vlastnosti zem. podloží vzhledem k dyn. úč. na staveb. konstrukce./ UTAM ČSAV Prague
- Kamenov, B. and Kysela, Z. /1979/. Selected problems of soil dynamics. /Vybrané problémy dynamiky zemin./ UTAM ČSAV, Prague
- Kysela, Z. and Fíft, V. /1974/. Shear failure on slip surfaces by dynamic load. Proc. 4th Danube European CSMFE, p. 193, Bled.

$$J_1 \cdot J_2 / J_3 = \text{const.} \quad (1)$$

$$\text{or } \tan^2 \phi_{mo12} + \tan^2 \phi_{mo23} + \tan^2 \phi_{mo13} = \text{const.} \quad (2)$$

where J_1 , J_2 and J_3 are the first, second and third effective stress invariants. Fig.2 shows the proposed failure criterion ($\tau_{SMP}/\sigma_{SMP} = \text{const.}$) and the measured values on the octahedral plane, obtained by true triaxial tests and conventional triaxial tests on the medium dense Toyoura sand (Nakai and Matsuoka, 1980). According to the proposed failure criterion, the maximum value of the internal friction angles ϕ_{max} is 10-15%

larger than those under triaxial compression and extension conditions, which are denoted by $\phi_{comp.}$ and $\phi_{ext.}$ ($\phi_{comp.} = \phi_{ext.}$). As ϕ_{max} corresponds nearly to the internal friction angle under

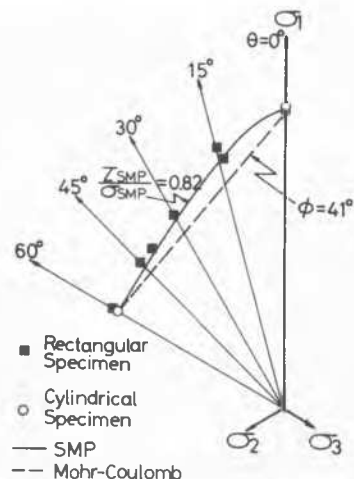


Fig.2 Proposed failure criterion and measured values on octahedral plane

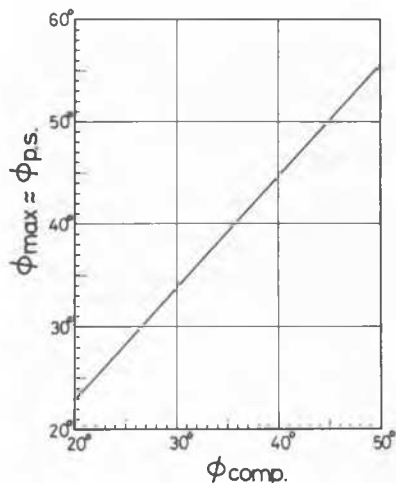


Fig.3 Calculated relationship between $\phi_{p.s.}$ and $\phi_{comp.}$.

T.L.L. Orr, D. Hartford and R.W. Kirwan (Written disc.)

THE EFFECTS OF PARTICLE SIZE DISTRIBUTION ON THE BEHAVIOUR OF TILL AS MEASURED IN THE LABORATORY

In our paper 4/39 to the conference we reported the results of a series of tests to investigate the influence of particle size distribution on the behaviour of till. The till tested is a granular material with less than 15% clay-sized particles of which mica predominates. The most common clay mineral is vermiculite and there are also small quantities of montmorillonite and kaolinite. High magnification photographs taken using a scanning electron microscope show that the silt-sized particles are rough and angular while the clay-sized particles are rough platelets.

The tests were carried out on samples of the till with different proportions of soil particles finer than 0.06mm. The samples were prepared to particular water contents using the same compactive effort. The test results presented in Table V of the paper show how the dry density and undrained shear strength parameters varied with changes in particle size distribution and water content.

The experimental results demonstrate that, for a particular water content or dry density, those samples with a higher proportion of fine particles had higher undrained shear strengths. Contrary to what the General Reporters suggest, this result confirms the findings of a similar investigation by Ostermayer (1979) who reported an increase in sample shear strength with increasing fines content.

The authors explain this result by considering the effect of changes in the particle size distribution on the behaviour of the soil matrix. For samples at the same density, a higher proportion of fine particles leads to a higher specific surface area and increased friction on shearing.

plane strain conditions $\phi_{p.s.}$, the relationship between $\phi_{p.s.}$ and $\phi_{comp.}$ can be calculated from Eq.(1) or (2). Fig.3 represents the calculated relationship between $\phi_{p.s.}$ and $\phi_{comp.}$, which will be useful for practical engineering designs of soil foundations under plane strain conditions.

REFERENCES

- 1) Matsuoka, H. and Nakai, T. (1974), Proc. of Japan Society of Civil Engineers, No.232, 59-70.
- 2) Matsuoka, H. and Nakai, T. (1977), Proc. of Specialty Session 9, 9th ICSMFE, 153-162.
- 3) Matsuoka, H. (1976), Soils and Foundations, Vol.16, No.1, 91-100.
- 4) Nakai, T. and Matsuoka, H. (1980), Proc. of Japan Society of Civil Engineers, No.303, 65-77, (in Japanese).

For the partially saturated samples tested under undrained conditions, an increase in the fines content also increases the capillary tension. Together these effects caused the observed increase in undrained shear strength with increasing fines content.

The experimental results also show that a reduction in the proportion of fine particles produced denser samples and an increase in the undrained shear strength. These samples had higher uniformity coefficients and greater particle interlocking. The increase in measured undrained shear strength in this case is due to the high degree of particle interlocking. The higher proportion of larger particles leads to increased dilatancy on shearing (Rowe 1962) and the negative pore water pressures developed do not equalise readily due to the dense nature of the soil matrix. This also caused an increase in the measured undrained shear strength.

Thus the authors conclude that the results of these experiments show two different effects arising from changes in the proportion of fine particles in a till.

REFERENCES

- Ostermayer, H. (1979) : Scherfestigkeit verdichteter Kies-Sand-Ton-Gemische. (The shear strength of gravel-sand-clay mixtures) Geotechnik 2, 140-147.
- Rowe, P.W. (1962) : The stress-dilatancy relation for static equilibrium of an assembly of particles in contact. Proc. Royal Soc. A, 264, 500-527.

A.M. Piaskowski (Written discussion)

With reference to my report "An attempt of new classification of cohesive soils" / Session 4 / I would like to explain the proposed principles of identification of soils. Figure 1 presented the classification of soils according to Polish Standard PN - 74 B - 02480 where in adequate fields are put symbols / Pg . . . I / of particular groups of soils. The dotted fields correspond to the soils which were investigated.

The axis "x" in the figure 2 is equal to values of

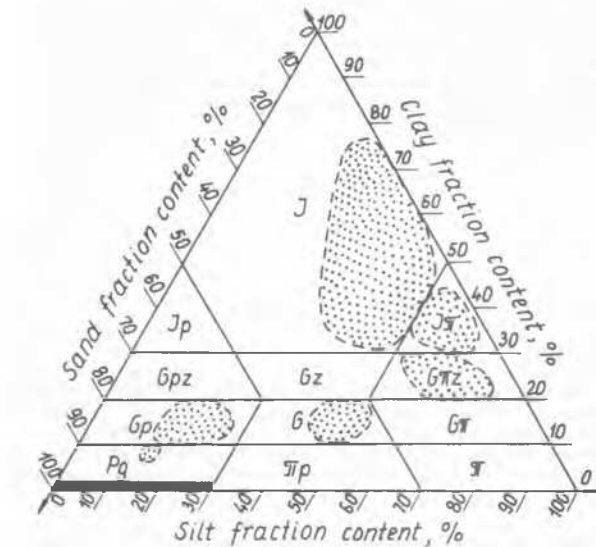


Fig. 1 The investigated soils according to the standard PN-74/B-02480.

J. Sigismund and M. Londez (Written discussion)

LA CRAIE ALTEREE - DEFORMATIONS DIFFEREES MESUREES EN LABORATOIRE

RESUME Pour l'étude d'un site nucléaire sur la craie, Electricité de France a fait analyser les déformations différées de la craie altérée. Les essais montrent que le phénomène est significatif même pour de faibles niveaux de sollicitation. En pratique, les déformations différées peuvent atteindre 40% du tassement de la couche concernée. (Réf.1) Fundamentals of Soil Behavior, J.K. Mitchell (Wiley)

Pour une centrale nucléaire Electricité de France a étudié les caractéristiques géotechniques de la craie. Il s'agit de craie sénéonienne (Crétacé Supérieur) qui est altérée sur environ 15 m d'épaisseur. On l'appelle improprement craie marneuse. La stratigraphie est définie par la Fig.1

L'altération est en fait constituée d'éléments de craie pratiquement pure, broyés et transformés en un matériau ayant la granularité d'un sable et gravier riche en silt. On sait que la craie est un assemblage de particules, nanno fossiles et particules néoformées, elles-mêmes poreuses d'où sa faible compacité ; malgré cela la résistance est assez élevée y compris pour le matériau altéré qui est non ar-

$I_s = I_C - 11\%$ and the axis "y" - to the sand fraction content / f_p / : the dotted fields correspond to the same soils, which are presented in the figure 1.

The comparison of both figures let us to suppose that it is possible to find a field in figure 2 for each field of the Feret's triangle shown in figure 1. The names of soil - groups stay unchanged. For other groups of soils the investigation are still continued.

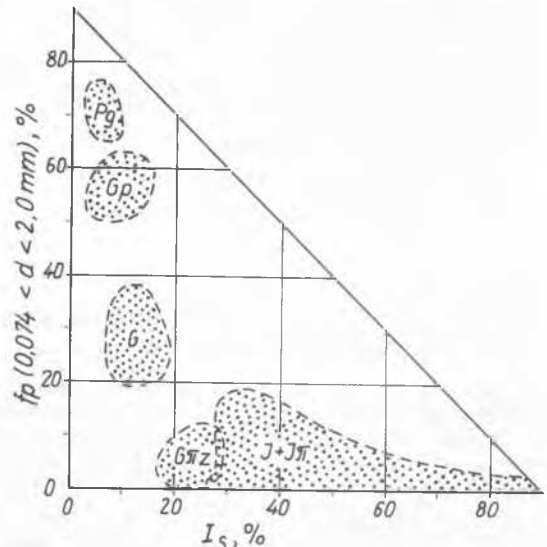


Fig. 2 The soils as in Fig. 1 acc. to proposed classification principles.

7,5 m 4 m 14 m > 100 m	$\gamma_d = 19 \text{ kN/m}^3$ $\gamma_s = 21 \text{ kN/m}^3$ $d_{10} = 0,4 \text{ mm}$ $d_{50} = 2 \text{ mm}$ $D_r = 80 \%$	CHARGE 470 kN/m ²	$C_d = 0$ $\sigma_d = 40^\circ$ $E = 125000 \text{ kN/m}^2$
	$\gamma_d = 15,5$ $\gamma_s = 20$ LL = 25 % LP = 19 % IP = 6 % CaCO ₃ = 98 %	ALLUVIONS SABLO-GRAVELEUSES	$E = 120000$ $C_{uu} = 200 \text{ kN/m}^2$ $\sigma_{uu} = 0$ $C_d = 80 \text{ kN/m}^2$ $\sigma_d = 36$ $\psi = 0,16$
	$\gamma_d = 16 \text{ kN/m}^3$ $\gamma_s = 20 \text{ kN/m}^3$ LL = 25 % LP = 18 % IP = 7 % CaCO ₃ = 99 %	CRAIE MARNEUSE CRAIE ROCHEUSE	$E = 800000 \text{ kN/m}^2$ $C_{uu} = 2000 \text{ kN/m}^2$ $\sigma_{uu} = 0$ $C_d = 700 \text{ kN/m}^2$ $\sigma_d = 36$ $\psi = 0,16$

Fig.1 Stratigraphie et caractéristiques du site

gileux, est très perméable. En phase de chargement, la dissipation de la pression interstitielle est très rapide.

LE FLUAGE : La craie est connue pour sa déformabilité différée sous charge.

Pour la craie rocheuse, le phénomène ne devient significatif que pour des déviateurs proches du déviateur de rupture.

Pour la craie altérée, le phénomène a une ampleur significative sous des déviateurs faibles.

Plusieurs séries d'essais ont été effectuées dans des cellules triaxiales pour divers niveaux de contraintes de confinement et pour des déviateurs croissants.

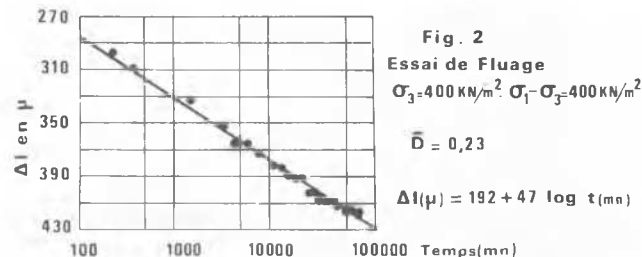
En se référant au paramètre :

$$\bar{D} = \sigma_1 - \sigma_3 / (\sigma_1 - \sigma_3)_{\text{rupt.}}$$

On a exploré le domaine $0,1 < \bar{D} < 0,5$ qui intéresse le projet étudié.

Les essais ont duré entre 2 et 3 mois, soit de 50 000 à 130 000 minutes.

La figure 2 présente les résultats d'un essai pour $\bar{D} = 0,23$, d'une durée de 2 mois.



A partir de l'ensemble des essais, une loi de comportement du type de celle proposée par le Professeur MITCHELL a été utilisée (Réf.1).

R. Stojadinović and M. Cvetković (Written discussion)

ANALYSIS OF VOLUME CHANGES ACCORDING TO THE CHANGE IN WATER CONTENT IN THE COHERENT SOILS

SYNOPSIS

In everyday's engineering practice it is often necessary to establish the soil volume changes when it is moistened or dried. It is especially important when the subsoils of roads or airport runways are considered, as well as in the cases of earthfill dams resp. their sealing cores. In such cases it is most important to be able to foresee the future behaviour of such materials, according to the moisture changes during the exploitation of such structures. The systematic research and testing showed that during the entire process of drying it is necessary to measure permanently the volume changes - and this being at the standard testing method impossible. It is proved influence on the shrinkage limit of the primary compactness of soil sample, and the moisture content at the beginning. It is stated too at testing that linear contraction (L_s) is not a constant value and dependent on the compactness at the start (γ_d), the moisture content (w), as well as of the disturbed soil structure and of some other soil properties.

In this paper is concentrated efforts on the study of volume changes in the soil with the changes of moisture content. The volume change is linear during the drying process from w_z to w_0 (Fig.1). The water is moving from the interior of the soil to the surface and evaporates up to the state when the relative air humidity reaches the value of 1,00. If the water in the soil is stressed, it ceases to evaporate earlier - before the relative moisture reaches the value of 1,00.

This lower value is marked as the relative pressure (h_r) of water vapour in the soil, the relation between the neutral pressure (u_w) and the relative pressure of water vapour (h_r) can be - in the limits of temperature from 10° up to 30°C and the limits of the relative pressure (h_r) from 0,7 up to 1,00 - expressed with the equation

$$u_w / \text{kN} = 150\,000 (1 - h_r).$$

For instance, if the value of h_r is equal to 0,9,

Selon la présentation classique des phénomènes de fluage (Fig.3), on observe la grande diminution de la vitesse de déformation avec le temps mais une faible variation de cette vitesse avec \bar{D} (Fig. 4).

VARIATION DE LA VITESSE DE DEFORMATION EN FONCTION :

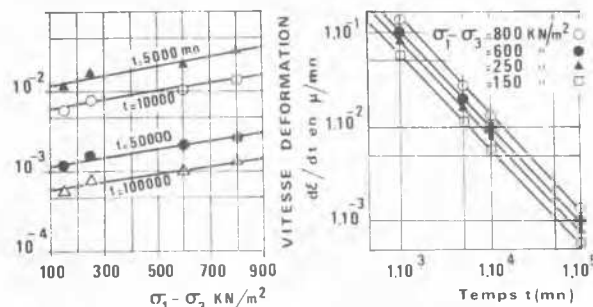


Fig. 3 DU DEVIEATEUR

Fig. 4 DU TEMPS

LES RESULTATS PRATIQUES :

La loi de fluage de la craie marneuse est :

$$\frac{\Delta \varepsilon}{\Delta} \% = 0,07 e^{1,6 \bar{D}} \log \frac{t}{t_f}$$

Cette loi a permis d'estimer les tassements différés sous les ouvrages étudiés.

La déformation différée représente environ 40 % du tassement total de la couche de craie altérée au bout de 30 ans (36 mm pour 91 mm).

Le phénomène est donc significatif pour des taux de cisaillement assez faibles.

then the value of u_w equals to - 15 000 kN/m². The water content in the soil does not remain constant unless the relative moisture of the nearby air is $h_{ra} = 0,9$. If the relative water vapour pressure h_r is lesser, the soil continues to lose the water by evaporation. With the later drying, the air enters into the cavities in the soil and the loss of water is lagrer than the volume change.

In this phase the water stress u_w can be increased, because the water retires to the finest pores. The evaporation does not cess as long as the relative vapour pressure h_r does not become equal to the relative moisture content h_{ra} . In this phase the shrinkage is called "the residual shrinkage". The structure, formed then, is resisting the forces of surface stresses, tending to diminish still more the soil volume in the continuous process of drying. This is the so called "residual resistance". The cross-points of the linear parts of the curve I gives the approximate value around the shrinkage limit (w_R). It is

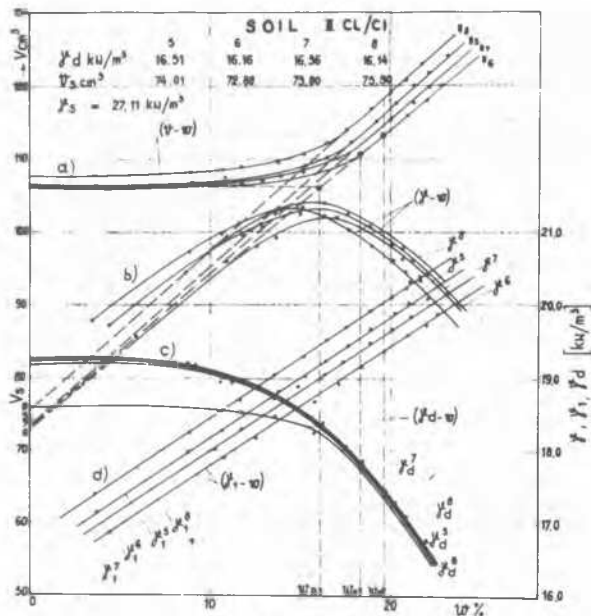


Fig. 1. V and γ_d , depending from the water content, $w\%$

possible to state, according to the diagram (Fig. 1) the following:

- For the same soil, and for the larger values of γ_d a smaller shrinkage limit is obtained (Fig. 1a).
- The diagram (γ_d - $w\%$) has the extreme value when the water content is w_R (Fig. 1b).
- The value of γ_d is changing approximately in a linear manner - from the start of drying up to the value of w_0 , as well as at the end of drying process, - i.e. it is inverse to the curve (V - $w\%$) - Fig. 1c.).
- The curve representing the weight by volume, related to the primary volume V , (γ_d - $w\%$) is linear (Fig. 1d).

The dependance of the linear change of volume (L_s as the function of primary compactness and of the water content at the standard Proctor's testing is examined too (Fig. 2 and 3).

On the Fig. 2 it is seen that the linear shrinkage change curve (No. I) in both cases is linear too,

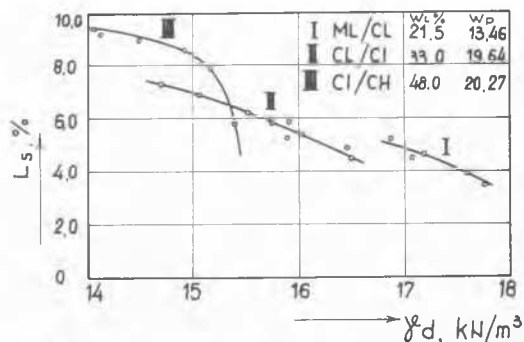


Fig. 2. The linear shrinkage change L_s as the function of γ_d and of $w\%$

but the value of L_s is growing much faster with the increase of water content on the right from the w_{opt} . At the part nearby around the optimal value of (L_s - $w\%$) the relation is no more linear. When the soil compactness is increasing relatively to the γ_d values, the change of L_s diminishes.

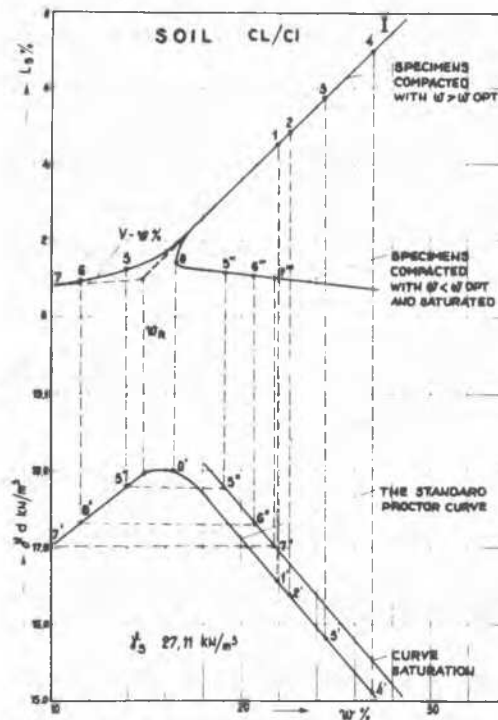


Fig. 3. The dependance of L_s from γ_d

The values of γ_d in natural conditions for the same material differ from the values, obtained when the experiment is performed in laboratory conditions, the structure is essentially different too.

The behaviour of the soil at the different states of consistency may be explained by the theory of osmotic pressure too, - this may be defined in the system soil/water by the expression

$$P = RT \frac{w}{w_a} f(w)$$

where are:

- R - the universal gas constant 0,082,
- T - absolute (Kelvin) temperature,
- " T " - the value of Hissic, or the capacity of the interchange of ions, expressed in the milliequivalents (me) on the 100g of the hard mass,
- w_a - the valency,
- w - the water content, equilibring the pressure p when the other conditions are the same,
- $f(W)$ - the coefficient of activity, expressing the actual, real osmotic ion activity under the existing environment conditions.

The osmotic pressure is a decreasing function of water content. It's maximal value corresponds

ding to the water content of w_0 and indicate the theoretical minimal water content at which the osmotic pressure starts to be formed.

The maximum practically coincides with the shrinkage limit for the Na^+ and K^+ of the clay considered ($w_0 = w_R$). The relation w_0/w_R is increased for the other ions. At the smaller water contents the capillar and polar forces disappear.

Rheological model of the state of saturated, not loaded soil at the relative humidity $h_{ra}=100\%$ is given on the (Fig. 4). The unique external force

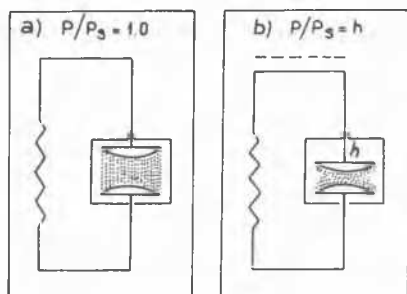


Fig. 4. The rheological model

is actually the atmospheric pressure. The swelling pressure, caused by repulsing forces is positive one and is equilibrated by the extension stresses in the hard part of the structure. On the (Fig. 4) the rheological model of this state is shown. The elastic spring is considered to be slightly stressed and the element of attraction is supposed to contain all adsorbed water and also that this water acts by the hydrostatic pressure on the grains of the soil. The water vapour pressure is equal to the vapour pressure at the saturation ($p/p_s=1$).

On the (Fig. 4b) the model is shown for the case when the pressure of water vapour in the nearby environment is reduced to a certain value h , part from the saturation condition, and when the entire system is in a state of balance. A certain quantity of water vapour is freed from the sample and is gone in the atmosphere. It is supposed that the water vapour pressure in every part of the sample is equalized and is equal to the pressure of the nearby environment. Consequently, then appear the surface stresses of the adsorbed wa-

ter-films, resp. the hydrostatic pressures are decreased, so that the soil structure (skeleton) starts to shrink, -i.e. to be compacted. This compacting is of a reversible character.

The soil characteristics, influencing this shrinkage were studied in the laboratory on some small samples, with a continuous following the progress of volume changes. The volume changes at the drying in situ can differ considerably from the values, found in the laboratory. Generally speaking, the volume changes in situ are lesser than these, found in the laboratory conditions. On the building site the climate is especially important in defining the gradient of volume changes. It is also important if the soil is covered (with grass etc.) or when it is not the case. The reversibility of shrinkage is depending from the activity of clayey minerals too (Fig. 5). Then the process of moistening and

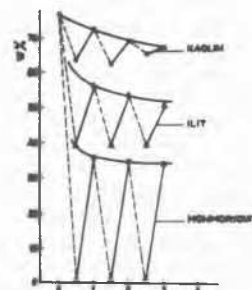


Fig. 5. The number cycles drying and moistening

of drying in the nature is cyclical - this influencing the final shrinkage value.

REFERENCES

- Bouche, M. (1967). Propriétés physiques et mécaniques des sols fins compactés, Annales ITB N° 240.
- Seed, H.B., Mitchell, J.K., Chan, C.K. (1960). The strength of compacted cohesive soil. A.S.C.E. Research conference on shear strength of cohesive soils.
- Stojadinović, R. (1972)., Mehanika tla I and II

Tan Tjong Kie (Written discussion)

LONG TERM STRENGTH: THEORY AND NEW SIMPLE METHOD OF DETERMINATION

For engineering purposes the long term strength i.e. the maximal stress which soils, rocks, interbedded clay layers and intercalations can sustain during the life of engineering constructions, is very important. In this discussion we will introduce a new method, which is very simple and has the great advantage that use can be made of the routine direct shear and or triaxial cell, which is available in every laboratory.

From a large quantity of creep or relaxation tests on rock, soils and interbedded clayey layers in rocks the stress strain (or displacement) isochrones for different values of the hydrostatic triaxial or normal pressures (direct

shear) have been found to have the form shown in Fig.1 (Geuze Tan 1953, Tan Kang 1980, Tan Lee 1981). This figure shows that for larger values of the time t the mutual distance between the isochrones become increasingly smaller and for very large values of the time the curves are squeezed into a narrow band. Creep tests at constant stress are shown in this diagram by horizontal lines CD whereas relaxation tests by vertical lines AB. The relaxation stress at large values of the time here is shown by the ordinate of the horizontal part of this band; its asymptotic value, which is the theoretical long term strength is here marked by σ_y or f_3 , the upper yield value. According to this

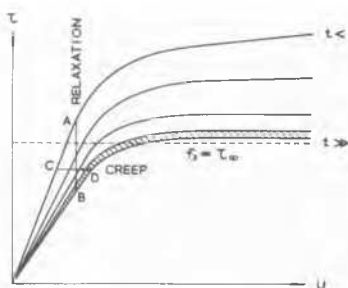


Fig.1 -u-t curves are squeezed to narrow band for large values of the time

reasoning, we can find the long term strength by determining the position of the narrow band in the stress strain diagram. We see that it is difficult to determine it by means of drawing horizontal lines CD, whereas it can unambiguously be determined by drawing vertical lines AB. Physically it means that it is difficult to find the long term strength by means of creep tests, whereas it can be determined from relaxation tests in a straight forward manner. Hence relaxation tests are preferable.

So to find the long term strength it is desired to measure the relaxation curves on the long term for different constant hydrostatic pressures or normal pressures. For this purpose we can use the common triaxial cell or direct shear box, only with some slight modifications i.e. we must be able to apply a constant strain and measure the stress relaxation with a very rigid dynamometer. Such a modification for example is shown in Fig.2. Typical relaxation curves for interbedded clay sheets are shown in Fig.3. From these group of curves the stress strain isochrones shown in Fig.1 can be directly obtained. Constant strain relaxation tests will require a large multitude of samples and for reasons of better efficiency the method of multiple step strainings is recommended (Tan Lee 1981) Fig.4 shows the results of a long term relaxation tests measured during a period of 427 days. It can be noticed that the stress decrease from 150 days to 100 years is only 8% of the stress magnitude at short term.

Relaxation tests results can be described by the following equations (Tan Lee 1981)

$$\tau(t) = Ku/(1+Bu) \left\{ 1 + A \log t/t_0 \right\}^{-\gamma} \quad (1)$$

V.K. Tokhi and T. Ramamurthy (Written discussion)

Discussion on "AN EVALUATION OF THREE DIMENSIONAL SHEAR TESTING" by: M.U. Ergunn, Vol. 1, p 593

In his interesting paper, the author has advocated the behaviour of a 'field element' without adequate justification. This discussion attempts to present and justify the behaviour of such an element.

In the following σ_c , σ_e and σ_p denote the drained strength in compression ($b=0$), extension ($b=1$) and plane strain [$b = (\sigma_2 - \sigma_3) / (\sigma_1 - \sigma_3)$].

Abbreviation CTA is used to denote conventional

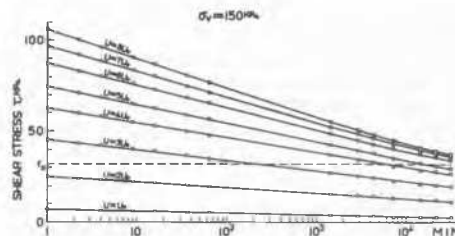


Fig.2 Typical results of Relaxation tests

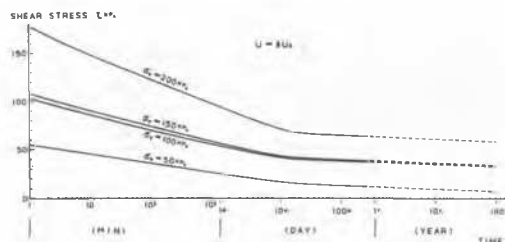


Fig.3 Relaxation curves 427 days

$$\sigma_{\text{Ku}}(1 - \dot{A} \log t/t_0) \quad (\dot{A} = \nu A) \quad (1B)$$

whereby: $K = K_0(\exp(\alpha \sigma_y))$; $K/B = (K/B)_0 + m \sigma_y$;

which are very usefull for the estimation of the long term value of the strength. For this purpose the experiments must be performed over a sufficiently long period that the coefficients K_0 , A , α , B , m can be determined satisfactorily.

REFERENCES

- Geuze, E,C.W.A and Tan Tjong Kie:"The mechanical Behaviour of Clays" Proc. 2nd Int. Congress Rheology, Oxford 1953 p247
- Tan Tjong Kie, Kang Wen Fa:"Locked in stresses, Creep and Dilatancy of Rocks and Constitutive Equations"; Rock Mechanics, 13,p5, 1980
- Tan Tjong Kie:"Relaxation and Creep Properties of Thin Interbedded Clayey Seams and Their Fundamental Role in The Stability of Dams" ISRM Int. Symp. Weak Rocks, Japan p..1981

triaxial apparatus, MCTA denotes axisymmetric triaxial compression test with lubricated end platens and UTA to denote an apparatus in which the three principal stresses and strains can be independently measured.

Until recently most of the study of strength and stress-deformation of soil depended on data obtained from CTA which uses a cylindrical specimen. Till about two decades back it was generally believed that $\sigma_p \approx \sigma_c$. When the plane

strain compression tests began to be performed, (Cornforth 1964), it was found that $\sigma_p > \sigma_c$. This was explained to be due to maximum constraint experienced by the specimen with $\epsilon_2 = 0$ resulting in σ_p to be maximum strength. It was also argued that in axisymmetric compression and extension tests in MCTA the specimen deforms under equal and maximum freedom in the two lateral directions and hence σ_c must equal σ_e . That $\sigma_c = \sigma_e$ is supported by several investigators, Rowe (1964), Bishop (1966), Marachi et al (1969), Barden et al (1969, 1971), using lubricated end platens. Later on several investigators using MCTA as well as UTA reported $\sigma_e > \sigma_c$. Green and Bishop (1969), Barden and Proctor (1971), Green (1971), Lade and Duncan (1973) and Green and Reades (1976). No reason could, however, be given for $\sigma_e > \sigma_c$. Though compression and extension tests may be conducted with identical preshear conditions namely porosity and confining pressure, the mean stress at failure in extension could be the same, higher or lower than in compression test and σ_e may be affected by this. This value of σ_e at failure may also be influenced by inherent anisotropy of the material. Sample geometry is not the cause for such a variation (Barden and Proctor, 1971).

From above it is clear that $\sigma_p > \sigma_c$ is generally accepted but magnitude of σ_e with respect to σ_c or with σ_p is not resolved and in the opinion of the discussors the basic question to be answered is: should σ_e obtained from MCTA or from UTA be taken as reliable? When comparison of σ_c obtained from MCTA and UTA was made, a good agreement was indicated. Whenever σ_e was determined from MCTA this value was less than σ_e obtained from UTA and also less than σ_p . One would expect the results in extension from MCTA, which provided near uniform deformation over the entire specimen under least deformational constraints to be more reliable. Some of the investigators have resorted σ_e to be

Table 1: Magnitude of σ_c , σ_e and σ_p

Author/s	Material	σ_c	σ_e	σ_p
Barden et al 1969	Dense sand	44.7	46.1	49.9
Green, 1971	Dense sand	39.0	40.9	44.0
Reades, 1972	Dense sand	38.8	43.2*	43.5
	Medium dense	37.0	38.6*	40.8
	Loose sand	34.0	33.7*	36.5
Thuraiajah and Sithamparapillai 1972	Dense	38.2	42.2	43.4**

* Middle of range for triaxial extension specimens.

** σ_p predicted according to Ramamurthy and Tokhi (1981).

a few degrees higher than σ_c from MCTA but less than σ_p as shown in Table 1.

In this Table, whenever σ_p has not been reported it has been estimated according to Ramamurthy and Tokhi (1981). In all these cases mean stress at failure in extension is higher than in compression and yet $\sigma_e < \sigma_p$. Adequate data is available to show that when mean stress at failure is constant or lower than in compression, $\sigma_e < \sigma_p$. UTA which have given $\sigma_e > \sigma_p$, must therefore be imposing some constraints in extension. Therefore, in all cases, σ_e should be less than σ_p . Some of the investigators have reported σ_e nearly equal to σ_c but less than σ_p from UTA e.g. Sutherland and Mesdary (1969) and Rawat and Ramamurthy (1978). Therefore, such UTA must be providing least equipmental constraints in extension as well. Therefore, from the data provided, in a "field element" at all relative densities the strength must increase from σ_c at $b = 0$ to its maximum value of σ_p under plane strain condition and with further increase in b it decreases to σ_e at $b = 1$ such that $\sigma_p > \sigma_e \geq \sigma_c$. For sand in loose state $|\sigma_e - \sigma_c|$ is expected to be small while in dense state it may be large, σ_p always remaining the maximum value.

For soils wherein $\sigma_p > \sigma_c$, $\sigma_e < \sigma_p$ and $\sigma_e \leq \sigma_c$

a new approach can be followed for defining a failure criteria in two stages in simple polynomial form after having experimentally determined σ_c and σ_e from MCTA and σ_p from an appropriate equipment (or estimated as explained earlier). The variation of σ in the region from $b = 0$ to $b = b_p$ ($b_p = b$ -value at plane strain) follows one type of polynomial behaviour and another type of polynomial in the region from $b = b_p$ to $b = 1$. Such a behaviour has been expressed in polynomial form (Ramamurthy, 1981; Tokhi, 1981). A major advantage of defining the failure criteria in this form almost individualises the failure criteria for each soil and the deviation of good and reliable experimental results from the failure criteria can be minimised.

References:

- Barden, L., Khayatt, A.J. and Wightman, A. (1969). Elastic and Slip Components of deformations of sand. Canadian Geotech. Jnl. Vol.6, No.3, 227-240.
- Barden, L. and Proctor, D.C. (1971). The drained strength of granular material. Canadian Geotech. Jnl. Vol.8, No.3, 372-383.
- Bishop, A.W. (1966). The strength of Soils as engineering materials (6th Rankine Lecture). Geotechnique Vol.16, No.2, 91-128.
- Cornforth, D.H. (1964). Some experiments on the influence of strain conditions on the strength of sand. Geotechnique, Vol.14, No.2, 143-167.

- Green, G.E. and Bishop, A.W. (1969). A note on drained strength of sand under generalized strain conditions. *Geotechnique*, Vol.19, No.1, 144-149.
- Green, G.E. (1971). Strength and deformation of sand measured in an independent stress control cell. *Proc. Roscoe Memorial Symposium*, Cambridge, 285-323.
- Lade, P.V. and Duncan, J.M. (1973). Cubical triaxial tests on a cohesionless soil. *J. Soil Mech. and Found. Div. ASCE* Vol.99, No.10, 793-812.
- Marachi, N. Chan, C.K., Seed, H.B. and Duncan, J.M. (1969). Strength and deformation characteristics of rockfill materials. Report TE-69-5, Univ. of California.
- Ramamurthy, T. (1981). Panel Report for Session 4, 10th Int. Conf. Soil Mech. and Found. Engg. (Stockholm) Vol.4.
- Ramamurthy, T. and Tokhi, V.K. (1981). Relation of triaxial and plane strain strengths. *Proc. 10th Int. Conf. Soil Mech. Found. Engg. (Stockholm)*. Vol.1, 755-758.
- Rawat, P.C. and Ramamurthy, T. (1978). Shear behaviour of sand under generalised condition of stress and strain. *J. Indian Geotech. Jnl.* Vol.8, No.4, 235-269.
- Reades, D.W. and Green, G.E. (1976). Independent stress control and triaxial extension tests on sand. *Geotechnique* Vol.26, No.4, 551-576.
- Rowe, P.W. (1964). Discussion on some experiments on influence of strain conditions on strength of sand. *Geotechnique* Vol.4, No. 361-364.
- Sutherland, H.B. and Mesdary, M.S. (1969). The influence of intermediate principal stress on the strength of sand. *Proc. 7th Int. Conf. Soil Mech. and Found. Engg. (Mexico)* Vol.1, 391-399.
- Thurairajah, A. and Sithamparapillai, V. (1972). Drained deformation characteristics of sand. *Geotechnical Engineering*, Vol.3, No.2, 91-104.
- Tokhi, V.K. (1981). Relationship between Strength and stress-strain behaviour in triaxial compression and plane strain, Ph.D. Thesis under submission to I.I.T. Delhi.

R.L. Wei, Y.M. Zuo and T.L. Guo (Written discussion)

CYCLIC SIMPLE SHEAR TEST APPARATUS

A cyclic simple shear test apparatus has been developed based on the original static simple shear test apparatus in Nanjing Hydraulic Research Institute since 1978. It is composed of four parts---simple shear box, static loading system, electro-magnetic actuator and electronic recording system. The main parts of this apparatus are shown in the left of Fig. 1, and the construction of the simple shear box is schematically illustrated in Fig.2. A specimen with diameter of 7 cm and height of 2 cm is enclosed inside a rubber membrane which is in turn confined by stack of steel rings and attached rigidly to the surfaces of the end plates by tapered sleeves with fastening bolts. It is shown by static test that under an inner pressure of 6 kg/cm² the shear box is completely water tight and no membrane inflation appears as there is not any unsupported section of membrane. A pressure transducer is installed at the pedestal

of the shear box to measure the pore pressure developed in the specimen during the test. An ancillary device is also provided to apply back pressure through the drainage line. The vertical and horizontal loads are applied pneumatically and controlled separately by two regulator valves. Vertical load is transmitted to the specimen through the load carriage fitted on the top cap of specimen and connected to a horizontally fixed small proving ring. When the horizontal cyclic load is applied, the load carriage is always kept horizontal with minimum rocking by guide ball bearings. The base of the shear box is connected with the loading rams of the horizontal pneumatic loader and electro-magnetic actuator which apply the initial and cyclic shear stress separately. Each of the loading rams is connected with a load cell

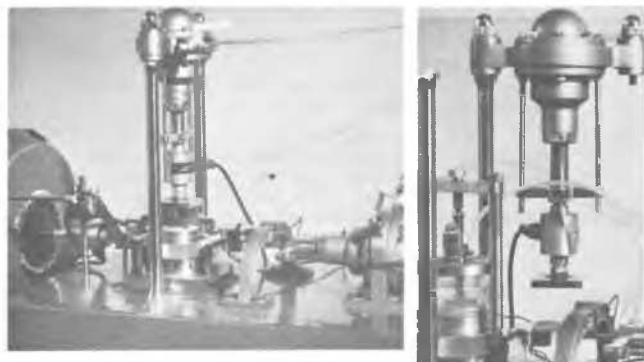


Fig.1 Cyclic Simple Shear Test Apparatus

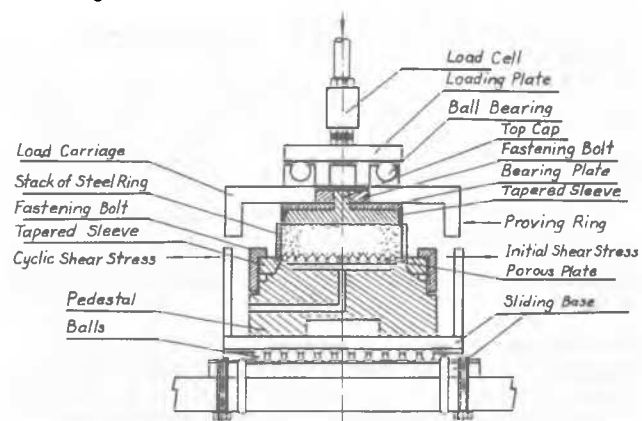


Fig. 2 Simple Shear Box

which monitors the intensity of the load transmitted to the specimen. The pedestal of shear box is mounted on a sliding base with a coefficient of friction of 2% determined by calibration. The magnitude and frequency of excitation is controlled by the extra-low frequency signal generator, the signal generated by the latter is amplified and input to the actuator. The maximum exciting force and stroke of the actuator is 120 kg and 20 mm respectively.

When there are too many fine grains in the sand that it is impossible to prepare the saturated specimen by boiling the test material and pouring it under the water, dry specimen is directly made in the shear box and then the air tight cell is mounted outside the shear box as shown in the right of Fig. 1. The valve of the drainage line on the base of the specimen is closed at first, and vacuum is applied from the top of the cell for 15 minutes. The valve is then opened slightly to let the water filtrating slowly through the specimen from the base until the water level in the cell has raised over the top surface of the specimen, and the vacuum is henceforth maintained for another 10 minutes. Caution must be taken that the filtration of water through the specimen should not be too rapid in order to avoid the disturbance of the placement structure of the specimen. It is shown by test that the degree of saturation of the specimen prepared with this procedure is generally higher than 97%.

After the specimen has been saturated, the air

W. Wolski/A. Fürstenberg/Z. Lechowicz/A. Szymański (Written disc.)

LABORATORY TESTS OF GEODRAIN EFFECTIVENESS IN ORGANIC SOILS

Soft organic layers in Poland comprise mainly of peat and gyttja. Such kind of soils covers about 5 per cent of the whole country. A typical soil profile with index and engineering properties are presented in fig.1.

For explanation of the stress-strain relationship of organic soft layers, scanning microscope as well as compressibility tests in the cells 15 cm dia. have been made. The above tests have shown that secondary compression in peat reached a value of about 30 per cent of total strains, whereas in gyttja only 10%. It was also found that coefficient of permeability decreases significantly under loading.

tight cell is dismantled, and the top cap is put on the surface of specimen. A special holder is constructed for the cap, allowing it to be lowered gently onto the specimen. When the rubber membrane is rolled and attached to the cap with tapered sleeve and fastening bolt, the cap is fixed temporarily to the holder, thereby preventing any vertical movement of cap and disturbance of the prepared specimen. When the vertical pressure has been applied to the specimen, the induced pore pressure is monitored before the drainage begins in order to check the degree of saturation of specimen. If the value of pore pressure coefficient B is less than 0.98, back pressure may be applied to the specimen to increase the degree of saturation.

When the specimen has been consolidated under the combined action of vertical pressure and horizontal shear stress, the drainage valve is closed, and the cyclic sinusoidal shear stress with a frequency of 2 Hz is applied by the electro-magnetic actuator. During the test the variations of cyclic shear stress, shear strain and pore pressure are measured by transducers and recorded by the oscilloscope.

Some of the preliminary results obtained with this apparatus has been summarized in a paper entitled "Pore Pressure in Silty Sand under Cyclic Shear" and published in the Proc. of the International Conference on Recent Advances in Geotechnical Earthquake Engineering and Soil Dynamics.

Due to obtained results: relatively small secondary compression and low permeability of gyttja, an attempt of assessment of effectiveness of geodrains in gyttja have been undertaken. The tests have been carried out in the two large scale concrete chambers (dimensions: 1.1 x 1.3 x 1.4 m); in one of them geodrain has been installed (fig. 2). Each chamber is provided with electrical piezometers and pipes for isotopic tests (water content and density). During the loading process the vane tests were available. The above tests were carried out under the loads 10, 20 and 30 kPa. Results of pore pressure measurements, settlements and vane shear strength are given in fig. 3.

Conclusions

Laboratory tests have shown that permeability of

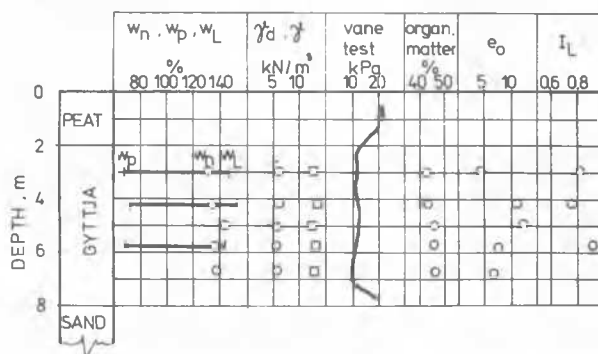


Fig. 1. Properties of the organic subsoil

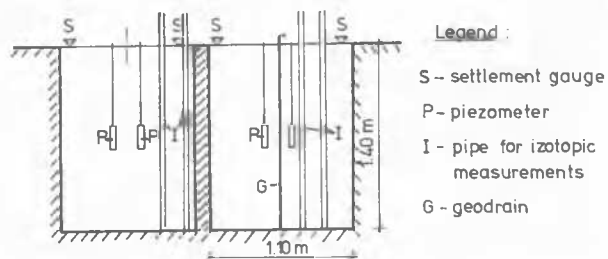


Fig. 2. Chambers of model test

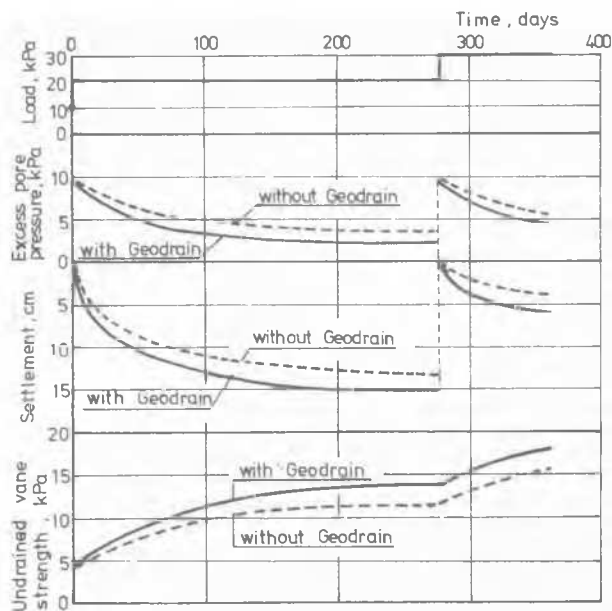


Fig. 3. Results of model test

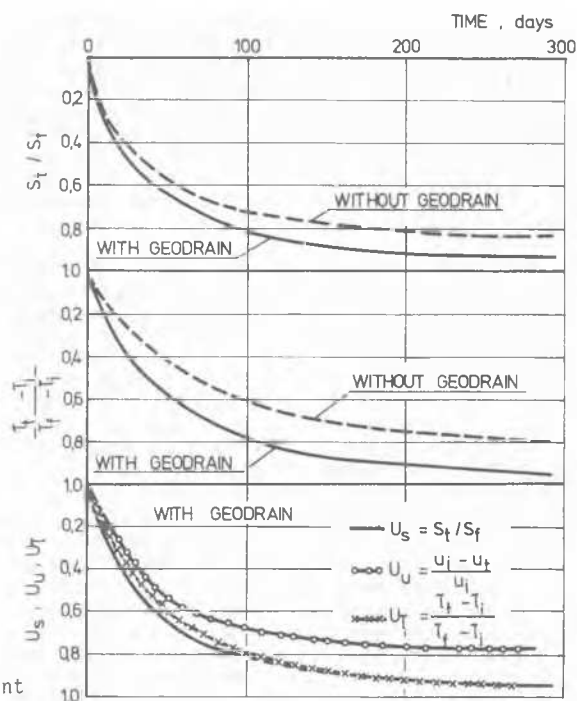


Fig. 4. Index of improvement

gyttja decreases 1000 times under the effective stress increase equal to 40 kPa.

Large scale model tests proved effectiveness of Geodrains, particularly in the further stage of consolidation. This effect comprising shortening of the con-

solidation time as well as increase of shear strength is presented in fig. 4.

It was also proved that the degree of consolidation treated as the degree of strains is higher than the degree of pore pressure dissipation.

F. Hartmann (Written discussion)

AN EVALUATION OF THE KJELLMAN TEST Une Evaluation d'un Essai de Kjellman

In 1936, Kjellman reported about his tests with the apparatus he had developed. Cubic soil samples are utilized. On each of the six side surfaces of the sample the stresses are applied via 100 brass rods. In this way a transfer of friction parallel to the load surfaces is avoided.

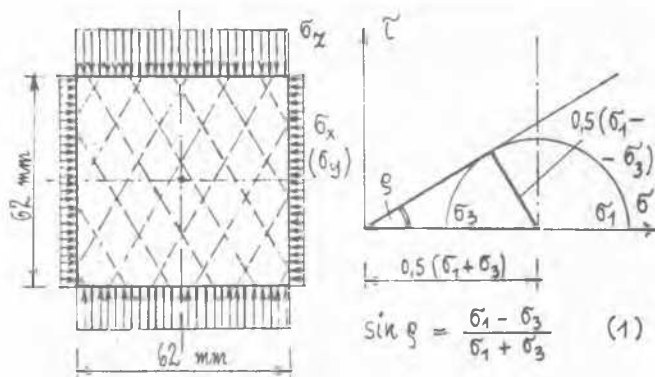


Fig. 1 a

Fig. 1 b

It can be assumed that the whole sample is submitted to uniform shear, see Fig. 1a, and that the evaluation of the results of the tests can be done as shown in Fig. 2b.

The results of Kjellman's tests are given in Table 1.

1	2	3	4	5	6	7
σ_x	σ_y	σ_z	x	ϵ_y	ϵ_z	e
2.27	6.00	12.00	-3.00	-0.20	+2.86	-0.34
1.87	6.00	10.13	-2.38	+0.20	+2.04	-0.14
2.65	2.65	9.70	-2.80	-2.80	+5.42	-0.18

Table 1

$$e = -\epsilon_x + \epsilon_y + \epsilon_z \quad (2)$$

It is assumed that the strain curves in (1) develop in a similar way and that, for the strain rates prevailing at the point of failure, the strain values can be employed, while the conversion factor, which is not needed for further calculation, is cancelled. Finally, the principal strain rates are calculated by the equation

$$\dot{\epsilon}_1 + \dot{\epsilon}_2 + \dot{\epsilon}_3 = 0 \quad (3)$$

Further calculation leads, by means of cyclical exchange, to the values given in the Table 2.

σ_1	σ_2	σ_3	$\dot{\epsilon}_1$	$\dot{\epsilon}_2$	$\dot{\epsilon}_3$	$\lambda = \frac{\sigma_2}{\sigma_3}$	$\frac{\dot{\epsilon}_2}{\dot{\epsilon}_3}$
6.00	2.27	12.00	-0.08	-2.89	+2.97	0.189	-0.973
6.00	12.00	2.27	-0.08	+2.97	-2.89	5.286	-1.028
2.27	6.00	etc.	-2.89	-0.08	etc.	0.500	etc.
1.87	6.00	10.13	-2.33	+0.24	+2.09	0.592	+0.115
1.87	10.13	etc.	-2.33	+2.09	etc.	1.688	etc.
2.65	9.70	2.65	-2.74	+5.48	-2.74	3.660	-2.000
9.70	2.65	2.65	+5.48	-2.74	-2.74	1.000	+1.000

Table 2

In Fig. 2, the values of σ_2/σ_3 calculated in Table 2 are plotted on the $\dot{\epsilon}_2'$ vs. $\dot{\epsilon}_3'$ plane.

The values in Fig. 2 can be expressed by a formula in the form

$$\ln\left(\frac{\sigma_2}{\sigma_3}\right) = (1.6766 - 0.7260 \sin \alpha - 0.9822 \sin^2 \alpha + 0.5941 \sin^3 \alpha) \cos \alpha \quad (4)$$

$$\text{with } \sin \alpha = \pm \frac{1 + \frac{\dot{\epsilon}_2'}{\dot{\epsilon}_3'}}{\sqrt{2[1 + (\frac{\dot{\epsilon}_2'}{\dot{\epsilon}_3'})^2]}} \quad \text{and} \quad (5)$$

$$\cos \alpha = \pm \frac{1 - \frac{\dot{\epsilon}_2'}{\dot{\epsilon}_3'}}{\sqrt{2[1 + (\frac{\dot{\epsilon}_2'}{\dot{\epsilon}_3'})^2]}} \quad (6)$$

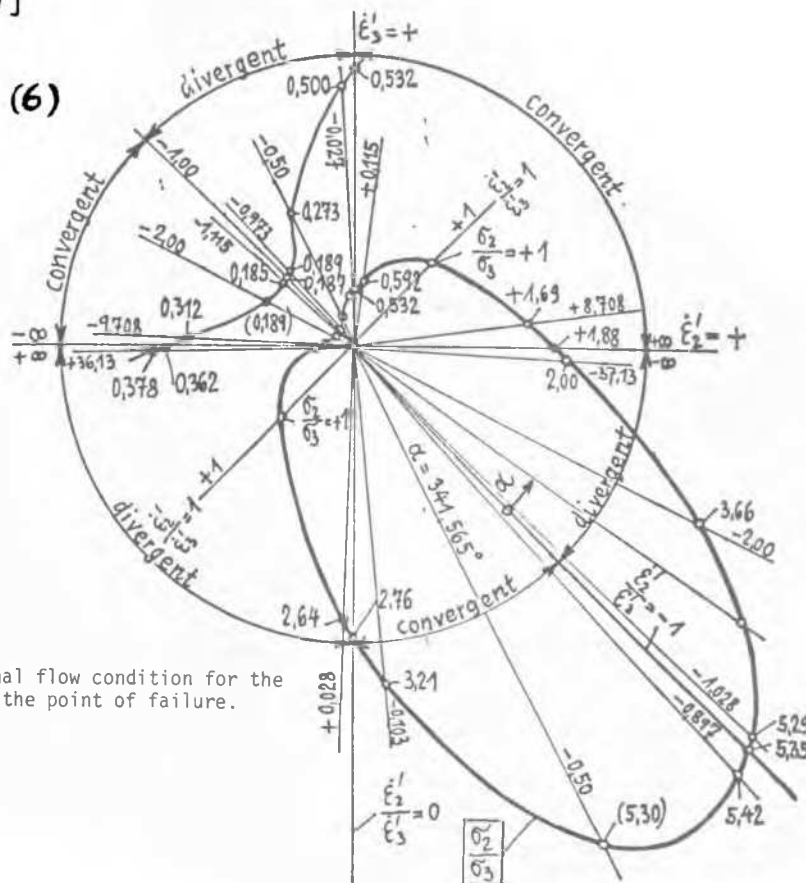


Fig. 2. Three dimensional flow condition for the tested sand at the point of failure.

The meaning of the angle α is to be seen in Fig. 2. By interpolation, some characteristic results are presented in Table 3.

	$\dot{\epsilon}_1'$	$\dot{\epsilon}_2'$	$\dot{\epsilon}_3'$	$\frac{\dot{\epsilon}_2'}{\dot{\epsilon}_3'}$	$\lambda = \frac{\sigma_2}{\sigma_3}$	$\lambda = \frac{\sigma_2}{\sigma_3}$	$\sin \vartheta$	ϑ
$\dot{\epsilon}_3'$	-1	0	+1	0	$\lambda_{0a} = 0.532$			
$\dot{\epsilon}_3'$	+1	0	-1	0	2.76			
$\dot{\epsilon}_3'$	0	-1	+1	-1	$\lambda_{2a} = 0.187$	$\lambda_{2p} = \frac{1}{0.187} = 5.35$	$\sin \vartheta_2 = 0.685$	$\vartheta_2 = 43.2^\circ$
$\dot{\epsilon}_3'$	-1	-1	+2	-0.5	$\lambda_{3da} = 0.273$	$\lambda_{3dp} = \frac{1}{0.273} = 3.66$	$\sin \vartheta_{3d} = 0.571$	$\vartheta_{3d} = 34.8^\circ$
$\dot{\epsilon}_3'$	+1	+1	-2	-0.5	$\lambda_{3kp} = 5.30$	$\lambda_{3ka} = \frac{1}{5.30} = 0.189$	$\sin \vartheta_{3k} = 0.683$	$\vartheta_{3k} = 43.0^\circ$

Table 3.

$$\sin \vartheta = \frac{1 - \lambda_a}{1 + \lambda_a} = \frac{\lambda_p - 1}{\lambda_p + 1}$$

At failure in the plane test the value $\rho_2 = 43.2^\circ$ and the parameter of side pressure $\lambda_{oa} = 0.532$ are obtained.

In the 3-dimensional case variable values which are dependent on the relationship of the strain rates are obtained.

In the case of uniform dispersion (divergent case) we find $\rho_{3d} = 34.8^\circ$ and in the case of uniform confluence (convergent case) $\rho_{3k} = 43.0^\circ$.

The great difference between the 3-dimensional case with $\rho_{3d} = 34.8^\circ$ and the 2-dimensional case with $\rho_2 = 43.2^\circ$ is remarkable. The flow process in the plane of the principal axes 2/3 is essentially facilitated if the soil grains are disturbed in a vertical direction to this plane.

From (1) it is to be seen the value of the linear compression at which the state of failure is not attained: $\lambda_o = 0.525$. It is approximately equal to the value $\lambda_{oa} = 0.532$. It is also interesting to compare the value $\lambda_o = 0.525$ with the values $\rho_{3d} = 34.8^\circ$ and $\sin \rho_{3d} = 0.571$. The formation of the pressure of repose is a 3-dimensional process like the divergent 3-way flow process. According to the formula of Jaky we can calculate [2]

$$\lambda_o = 1 - \sin \rho = 1 - 0.571 = 0.429$$

and according to a formula derived by the Author [2]

$$\lambda_o = \frac{1 - \sin^2 \rho}{1 + \sin^2 \rho} = \frac{1 - 0.571^2}{1 + 0.571^2} = 0.508. \quad (9)$$

The better coincidence according to my formula be thus explained. In my formula the value of the internal friction

angle must be introduced but in the formula of Jaky, however, the shear angle. Here a rough conversion for little or no volume change leads to

$$\begin{aligned} \tan \phi &\cong \sin \rho \\ \tan \phi &= \sin 34.8^\circ \end{aligned} \quad (10)$$

$$\begin{aligned} \phi_{3d} &= 29.7^\circ \\ \lambda_o &= 1 - \sin \phi = 1 - 0.496 = 0.504. \end{aligned} \quad (11)$$

Kjellman tested the sand in his apparatus and also in the Krey shear apparatus and found the value $\phi_2 = 34^\circ$. By the shearing test, the Mohr internal friction angle ρ was not to be found but the Coulomb shear angle ϕ .

If a volume change is not considered, the rough conversion from the shear angle leads to

$$\begin{aligned} \tan \phi_2 &= \tan 34^\circ = 0.6745 \\ \sin \rho_2 &= 0.6745 \\ \rho_2 &= 42.4^\circ \end{aligned}$$

and to a surprisingly good agreement with the value

$$\rho_2 = 43.2^\circ.$$

References

- [1] Kjellman, W. (1936). Report on an apparatus for consummate investigation of the mechanical properties of soils. Proc. 1. Int. Conf. Soil Mech. a. Found. Engng., Harvard University, Cambridge, Mass., Vol. 2, 16-20.
- [2] Hartmann, F. (1967). Die Berechnung des Ruhedruckes in kohäsionslosen Böden bei waagerechter Oberfläche. Die Bautechnik 11, 382-385.